World Journal of Clinical Oncology

Submit a Manuscript: http://www.wjgnet.com/esps/
Help Desk: http://www.wjgnet.com/esps/helpdesk.aspx
DOI: 10.5306/wjco.v5.i5.824

World J Clin Oncol 2014 December 10; 5(5): 824-844
ISSN 2218-4333 (online)

TOPIC HIGHLIGHT

WJCO 5th Anniversary Special Issues (1): Lung cancer

Positron emission tomography to assess hypoxia and perfusion in lung cancer

Eline E Verwer, Ronald Boellaard, Astrid AM van der Veldt

Eline E Verwer, Ronald Boellaard, Department of Radiology and Nuclear Medicine, VU University Medical Center, 1007 MB, Amsterdam, The Netherlands
Astrid AM van der Veldt, Department of Internal Medicine, VU University Medical Center, 1007 MB, Amsterdam, The Netherlands
Author contributions: Verwer EE and van der Veldt AAM designed and wrote the review article; Boellaard R contributed substantially to the design of the article; all authors critically revised the manuscript and approved the final version for publication.
Supported by AIRFORCE Project, No. 03O-103
Correspondence to: Astrid AM van der Veldt, MD, PhD, Department of Internal Medicine, VU University Medical Center, PO Box 7057, 1007 MB, Amsterdam, The Netherlands. aam.vanderveldt@vumc.nl
Telephone: + 31-20-4444444 Fax: +31-20-4443090
Received: January 30, 2014 Revised: April 29, 2014
Accepted: July 15, 2014
Published online: December 10, 2014

Abstract

In lung cancer, tumor hypoxia is a characteristic feature, which is associated with a poor prognosis and resistance to both radiation therapy and chemotherapy. As the development of tumor hypoxia is associated with decreased perfusion, perfusion measurements provide more insight into the relation between hypoxia and perfusion in malignant tumors. Positron emission tomography (PET) is a highly sensitive nuclear imaging technique that is suited for non-invasive *in vivo* monitoring of dynamic processes including hypoxia and its associated parameter perfusion. The PET technique enables quantitative assessment of hypoxia and perfusion in tumors. To this end, consecutive PET scans can be performed in one scan session. Using different hypoxia tracers, PET imaging may provide insight into the prognostic significance of hypoxia and perfusion in lung cancer. In addition, PET studies may play an important role in various stages of personalized medicine, as these may help to select patients for specific treatments including radiation therapy, hypoxia modifying therapies, and antiangiogenic strategies. In addition, specific PET tracers can be applied for monitoring therapy. The present review provides an overview of the clinical applications of PET to measure hypoxia and perfusion in lung cancer. Available PET tracers and their characteristics as well as the applications of combined hypoxia and perfusion PET imaging are discussed.

Key words: Molecular imaging; Positron emission tomography; Hypoxia; Perfusion; Quantification; Lung cancer

Core tip: This review provides an overview of the current applications of positron emission tomography for hypoxia and perfusion imaging in lung cancer. Available PET tracers are discussed and the benefits of combined hypoxia and perfusion PET imaging are clarified. Hypoxia imaging could aid in selecting patients for hypoxia-specific treatment strategies. To achieve this, consensus about the optimal imaging protocol and quantification method is essential. Large clinical trials are needed to confirm the value of hypoxia imaging for improving patient care.

Verwer EE, Boellaard R, van der Veldt AAM. Positron emission tomography to assess hypoxia and perfusion in lung cancer. *World J Clin Oncol* 2014; 5(5): 824-844 Available from: URL: http://www.wjgnet.com/2218-4333/full/v5/i5/824.htm DOI: http://dx.doi.org/10.5306/wjco.v5.i5.824

INTRODUCTION

Worldwide, lung cancer is the most common cause of cancer related death among men and women[1]. Every year, approximately 1.2 million new cases of lung cancer

are diagnosed globally and 1.1 million patients die of this disease[2]. Non-small cell lung cancer (NSCLC) and small cell lung cancer (SCLC) are the main histological types and represent approximately 85% and 15% of the lung cancer cases, respectively[3,4]. The prognosis of both NSCLC and SCLC is poor and depends on the stage of the disease[5,6]. For example, the 5-year overall survival is approximately 1% and 2% for stage Ⅳ NSCLC and extensive stage SCLC, respectively. Treatment of lung cancer depends on histological type, stage and performance status. The available treatment options include surgery, radiation therapy and chemotherapy, or a combination of these modalities. Systemic therapy of lung cancer consists mainly of a platinum-based doublet, such as cisplatin or carboplatin, in combination with a third generation cytotoxic drug such as gemcitabine, pemetrexed, paclitaxel or docetaxel[7,8]. In addition, targeted agents, including gefitinib, erlotinib, bevacizumab and crizotinib, have been introduced for the treatment of advanced NSCLC[9-16]. For the last decades, several tumor characteristics have been under investigation in order to further understand the biology of lung cancer and enhance the efficacy of the several treatment modalities.

In lung cancer, tumor hypoxia is a characteristic feature[17], which is associated with a poor prognosis[18-20] and resistance to both radiation therapy[21] and chemotherapy[22]. Hypoxia is a reduced O_2 tension in tissue and is defined between normoxia (pO_2 levels of 40-60 mmHg) and anoxia (0 mmHg)[23]. In clinical practice, no consensus has been achieved for hypoxic thresholds in tumors, but tumors with pO_2 values below 10 mmHg are usually considered hypoxic[23]. Tumor hypoxia is the result of an imbalance between oxygen supply and consumption and can be caused by the following mechanisms[23]: (1) the structurally and functionally abnormal tumor vasculature leads to a perfusion-limited delivery of oxygen[24], thereby inducing "acute" hypoxia; (2) tumor proliferation increases the distance between tumor cells and blood vessels that provide nutrients and oxygen to tumor cells. Consequently, the distances to blood vessels can become larger than the diffusion distance of oxygen (> 70 μm), locally causing diffusion-limited hypoxia (referred to as "chronic" hypoxia); (3) tumor hypoxia is also associated with a systemic decrease in oxygen supply, *i.e.*, anemia, which can be caused by tumor-related factors as well as anticancer therapy.

To promote cell survival in hypoxic conditions hypoxia inducible factor-1 (HIF-1) is upregulated, which in turn activates a number of processes including growth factor signaling, angiogenesis, proliferation, glycolysis, tissue invasion, and finally metastasis[25]. As a result, markers of the HIF signaling cascade such as HIF-1α, glucose transporter-1, and vascular endothelial growth factor (VEGF), have been investigated as surrogate markers for tumor hypoxia in lung cancer[18,19,26,27]. Alternatively, immunohistochemical staining using injectable exogenous bioreductive markers like pimonidazole and 2-(2-nitro-1[*H*]-imidazol-1-yl)-*N*-(2,2,3,3,3-pentafluoropropyl)-acetamide (EF5) can be applied[28]. However, immunohistochemistry requires tissue samples and represents an indirect measurement of tumor hypoxia. Alternatively, pO_2 levels in tumors can be directly assessed using Eppendorf polarographic electrodes. This an invasive technique that can be applied in tumors that are easily accessible[29]. In lung cancer, this technique is not feasible[17], as these tumors are usually deeply seated within in de body. Positron emission tomography (PET) may be useful, as PET enables direct assessment of tumor hypoxia in patients non-invasively[30].

As the development of tumor hypoxia is associated with decreased perfusion, perfusion PET imaging may provide more insight into the relation between hypoxia and perfusion in malignant tumors. PET scans may not only reveal the prognostic significance of hypoxia and perfusion in lung cancer, but may also help to select patients for specific treatments including radiation therapy, hypoxia modifying therapies, and antiangiogenic drugs[31,32]. This review provides an overview of the clinical applications of PET to measure hypoxia and perfusion in lung cancer.

PET PRINCIPLES

PET enables non-invasive 3D imaging of dynamic processes *in vivo*. To this end, molecules of interest are radiolabeled with positron emitting radionuclides. For PET imaging, commonly used radionuclides are oxygen-15 (^{15}O), carbon-11 (^{11}C) and fluorine-18 (^{18}F). These radionuclides are isotopes of elements that are often naturally present in organic molecules as well as in chemically produced molecules, *e.g.,* anticancer drugs. After replacing one of the molecules' atoms by its radioactive isotope, the molecular structure is unchanged, leaving chemical properties unaffected. After intravenous injection of a PET tracer, the radiolabeled molecules can be located within the body by detecting the emitted photons. Since only a small amount of radiotracer is required for PET imaging, it is assumed that the radiotracer does not affect the dynamic process under study.

PET is based on the detection of positron emission. During radioactive decay, the radionuclide, *e.g.,* ^{18}F, emits a positron which, after traveling a short distance (few mm) in tissue, annihilates with a nearby electron to emit two 511 keV photons in opposite directions. These two "annihilation" photons are registered by the PET scanner using a coincidence detection circuitry, providing 3D information of the tracer distribution with high sensitivity and resolution. To achieve quantitative accuracy, imaging data needs to be corrected for attenuation: when emitted from tissues deeper in the body, photons are more likely to be absorbed than from superficial structures. As a result, 3D images would falsely show low tracer concentrations in deeper structures compared to superficial structures. In PET, the attenuation perceived by the annihilation photon pairs, traveling in opposite directions over a line through the body, is mathematically equivalent

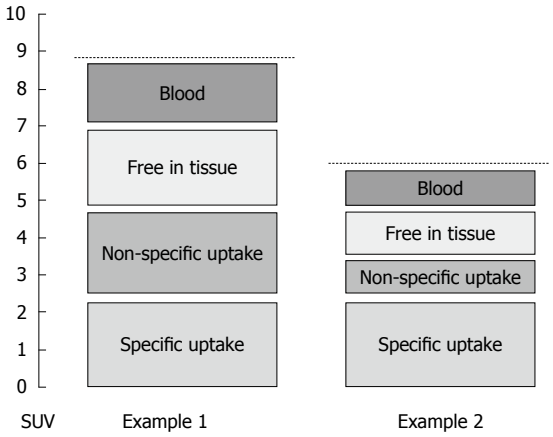

Figure 1 Graphical representation of the different components that determine the total positron emission tomography signal. Examples 1 and 2 can represent either different patients, different lesions in one patient or different scans of one patient, for example before and after therapy. In both examples the contributions of specific uptake (the uptake of interest) are equal, but the total signal is different due to differences in contribution of other (non-relevant) signals. Measured standardized uptake value (SUV) values are reflected by the dashed lines. As SUV does not only reflect the specific signal, its use should be validated before it is used in a clinical setting, *i.e.*, it is required to assess if contributions from non-specific signals affect SUV values in a non-predictable way. For the purpose of illustration, the Y-axis represents SUV values on an arbitrarily chosen scale.

to the attenuation perceived by one photon transmitted through the body over that same line. Therefore, accurate attenuation correction can be achieved using a transmission source, *e.g.*, computed tomography (CT). In addition, PET/CT systems can correct for false detections due to random coincidence detection or scattered annihilation photons. As a result, PET provides radioactivity measurements with high quantitative accuracy[33].

Quantification of tracer uptake, however, remains challenging. First, the measured radioactivity concentration in tissue depends on the tracer concentration in blood over time, which, in turn, depends on the injected dose and distribution volume. The standardized uptake value (SUV) takes this variability into account, as the radioactivity concentration in tissue is normalized by the ratio of the injected dose to patient weight. Second, the PET signal does not necessarily reflect specific uptake, *e.g.*, trapping of the tracer by the process of interest. A tracer could also be free in tissue, trapped by a different process or reside in blood vessels within the region of interest, *e.g.*, tumor (Figure 1). Pharmacokinetic modeling can be applied to distinguish between the various kinetic processes and separates the total signal into these components[34].

In addition to spatial information, temporal information of the tracers' distribution is used in pharmacokinetic modeling. To obtain information on the changes in tracer activity concentrations over time (time activity curves or TAC), sequential PET images are acquired over the same body area. In addition, accurate temporal data on tracer concentration in plasma is obtained from arterial blood sampling and dedicated lab analysis. Mathematical models ("compartment models") are then used to extract measures of the relevant components of the tracers' kinetics, such as specific uptake or binding. As absolute quantification by kinetic modeling can be challenging and cumbersome in the clinic, alternatives have been introduced to measure tracer uptake. Before clinical implementation, these "simplified parameters" (such as SUV) should be validated and correlated with parameters from pharmacokinetic modeling.

To date, 2-deoxy-2-[^{18}F]fluoro-D-glucose ([^{18}F]FDG) is the most commonly used PET tracer. As [^{18}F]FDG is a glucose analogue, it accumulates in malignant tumors with high glucose consumption. As a result, [^{18}F]FDG PET is extensively used for diagnosis, staging and response monitoring of cancer. Currently, [^{18}F]FDG PET is routinely performed for initial staging[35] and pre-operative staging[36,37] of patients with NSCLC. As tumor hypoxia is associated with increased glycolysis, it is conceivable that hypoxia is associated with increased [^{18}F]FDG uptake. However, results on [^{18}F]FDG to assess tumor hypoxia have been conflicting[38], indicating that [^{18}F]FDG is not specific enough to identify hypoxia. Therefore, other PET tracers have been developed to measure hypoxia and perfusion in tumors more specifically. In the following paragraphs, these PET tracers will be discussed.

TUMOR HYPOXIA IMAGING

Clinical relevance

Tumor hypoxia is associated with resistance to both radiation therapy[21] and chemotherapy[22]. Radiation therapy requires oxygen to induce DNA damage and hypoxic cancer cells are three times less sensitive to radiation therapy than normoxic cancer cells[39,40]. In addition, the resistance to anticancer drugs is attributed to the lack of O_2 available for drug activation, the increased genetic instability, the antiproliferative effects of hypoxia, and the increased gene transcription induced by HIF-1[41,42]. Currently, drugs that selectively target tumor hypoxia and its increased gene transcription are still under study and have entered the first clinical trials[43-45]. Since tumor hypoxia may affect clinical outcome, hypoxia imaging may be useful to determine prognosis and tumor response in lung cancer patients. Furthermore, hypoxia assessment may help to optimize treatment strategies in individual patients.

In particular, the efficacy of radiation therapy may be increased by several interventions. First, the systemic oxygenation level can be increased by hyperbaric chamber treatment[46], carbogen breathing[47] and improved oxygen transport by hemoglobin. For the latter, blood transfusions and erythropoietin injections are available[48]. Oxygen transport can be further improved by agents that improve perfusion and affect vascular permeability[49]. Second, the apparent oxygenation level in tumors can be increased using radiosensitizers, which are usually based on a nitroimidazole-group and specifically target hypoxic tumor cells ($pO_2 < 10$ mmHg). Once incorporated in hypoxic tumor cells, radiosensitizers mimic oxygen, thereby

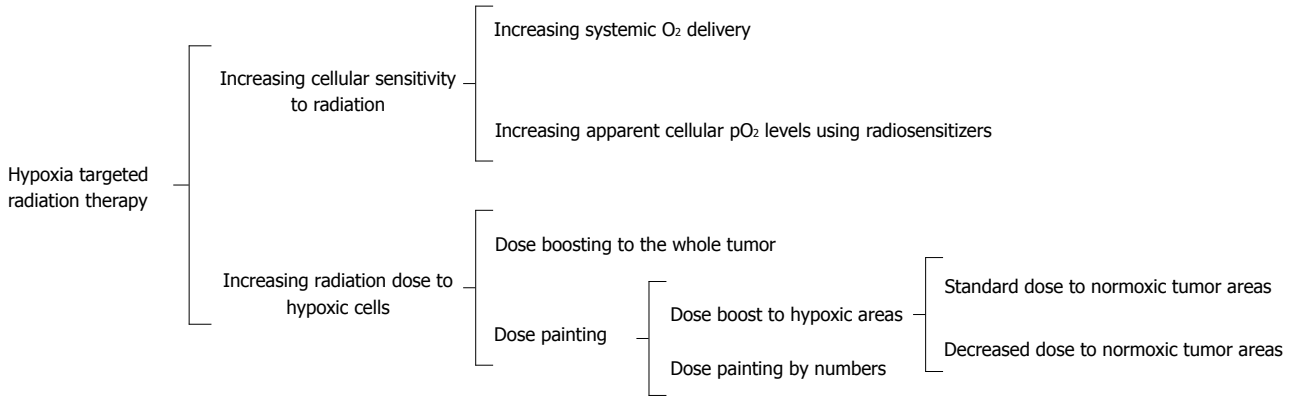

Figure 2 Radiation therapy treatment strategies for tumor hypoxia.

increasing the efficacy of radiation therapy[50]. Third, the radiation therapy plan can be adjusted to increase the dose administered to hypoxic tumor tissue. This can be achieved by dose boosting to the whole tumor, dose painting, or dose painting by numbers[51]. For dose boosting, an increased dose is administered to hypoxic areas, thereby increasing the radiation dose to normal tissue and, potentially, its associated side effects. For dose painting, the dose to a specific area (*e.g.*, hypoxic area) is increased, whereas the radiation to the remaining part of the tumor can be either maintained or decreased. In the latter case the total dose level can be maintained. Dose painting can be further refined when it is directly based on the voxel-by-voxel values of a PET image (referred to as "dose painting by numbers"). For successful implementation of the previous mentioned radiation therapy strategies, hypoxia imaging may help to identify hypoxic tumors, prevent unnecessary side effects in patients with normoxic tumors, and reveal heterogeneous distribution of hypoxia within tumors. Figure 2 summarizes the potential applications of hypoxia imaging for radiation therapy.

Characteristics of a hypoxia PET tracer

The ideal hypoxia tracer would freely and rapidly diffuse to tissue, including remote areas. For optimal contrast of the PET image, accumulation of the tracer should be high in hypoxic cells, whereas no binding should occur in normoxic cells. To achieve the best image quality, an optimal balance between tracer half-life, accumulation rates and clearance rates is required: the tracers' half-life should be long enough to obtain a high signal-to-noise ratio whilst allowing the tracer enough time to diffuse and bind to hypoxic cells and clear from normoxic tissues and blood. Accumulation and clearance rates are influenced by the tracers' octanol/water partition coefficient. More lipophilic compounds may more readily pass through the cell membrane. On the other hand, more hydrophilic compounds may more easily diffuse across tissues and show faster clearance from blood and normoxic tumors through the urinary pathway[30,52]. Besides these hypoxia specific characteristics, the tracer should be metabolically inert, since the formation of radiolabeled metabolites results in a decreased amount of the original tracer available for hypoxia specific uptake, poor image contrast and inaccurate tracer quantification.

For clinical implementation, hypoxia tracers require fast kinetics, allowing for rapid accumulation in hypoxic tissues, thereby limiting the time between tracer injection and imaging. In addition, simplified and reproducible methods (*e.g.*, SUV) are needed to quantify tracer uptake.

Hypoxia tracers for PET

Over the last decades, several PET tracers have been developed to measure tumor hypoxia. To identify all relevant hypoxia tracers in lung cancer, a literature search was conducted in PubMed to identify studies published before 1 January 2014. To this end, PET specific search terms (PET, positron emission tomography) were combined with hypoxia specific search terms (hypoxia, anoxia), and/or lung cancer specific search terms (lung cancer, lung neoplasms, non-small cell lung cancer, small cell lung cancer), and/or kinetic modeling specific search terms (kinetic modeling, modeling), and/or radiation therapy specific search terms (radiation therapy, radiation). For these search terms, the corresponding Mesh terms were included. Thereafter, the obtained English abstracts were evaluated for relevance. Based on the obtained publications, a specific search strategy was subsequently performed for each identified hypoxia PET tracer. Additional publications were identified by cross-referencing. Brain studies were excluded since the blood-brain barrier may affect tracer kinetics. Figure 3 and Table 1 give an overview of the identified hypoxia tracers that have been evaluated in oncology. The tracer names and abbreviations are displayed in Table 2. These hypoxia tracers can be subdivided in nitroimidazole-based and thiosemicarbazone-based tracers. In the following paragraphs, these tracers and their potential applications in lung cancer patients will be discussed.

Nitroimidazole-based tracers: Originally, nitroimidazoles have been developed as radiosensitizers. Already in 1984, Chapman[53] have proposed nitroimidazoles for

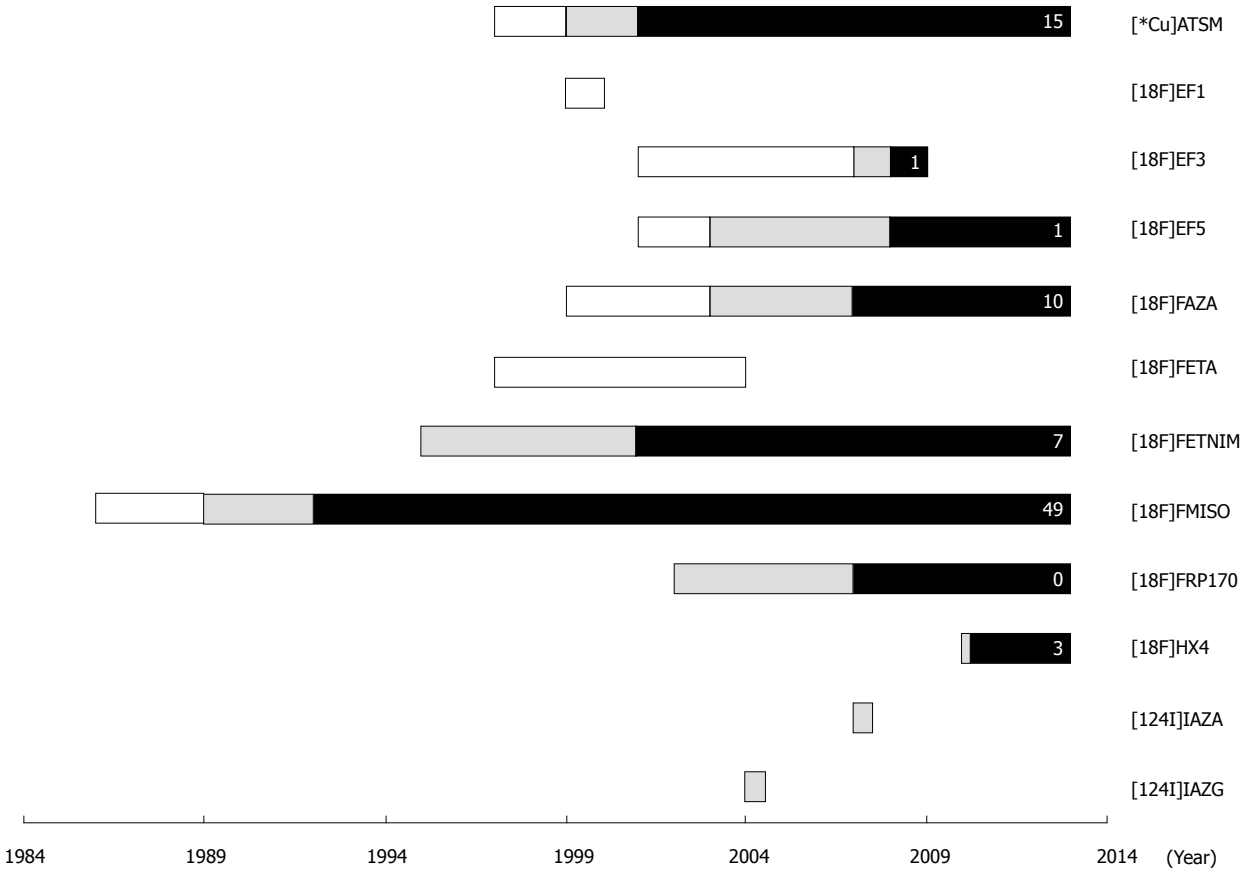

Figure 3 Timeline for development and evaluation of hypoxia specific tracers that have been evaluated by preclinical or clinical positron emission tomography. Development and *in-vitro* analysis (blank), preclinical positron emission tomography (PET) evaluation (grey), and clinical PET evaluation (black). The number of published clinical studies in oncology is indicated (excluding brain studies). See Table 2 for full names.

hypoxia imaging. Upon entering the cell, nitroimidazole undergoes electron reduction, thereby becoming a radical. In normoxic cells, this reaction is reversed by O_2. In hypoxic cells, the radical can react with an intracellular macromolecule instead and remains trapped. As the latter process occurs at $pO_2 < 10$ mmHg, an oxygenation level associated with increased radiation therapy resistance, nitroimidazoles are able to detect clinically relevant hypoxia[54].

Among the developed hypoxia tracers for PET (see Figure 3), [^{18}F]FMISO has been investigated most extensively. Although [^{18}F]FMISO showed rapid metabolism in mice studies, it appeared to be a robust hypoxia tracer in humans, with parent fractions up to 96% at 90 min after injection[55]. Since [^{18}F]FMISO is rather lipophilic with a partition coefficient (log P) of 0.4, clearance from blood and normoxic tissues is slow. Therefore, the required time intervals between injection and imaging are long, at least 3 h[56]. Efforts have been made to develop hypoxia tracers with more favorable characteristics. Being the most evaluated and validated hypoxia tracer to date, the performance of new hypoxia tracers is often compared with [^{18}F]FMISO (see Table 1). Among these tracers, [^{18}F]FAZA has been introduced in the clinic. [^{18}F]FAZA (log $P = 0.04$) is more hydrophilic than [^{18}F]FMISO and shows faster clearance from blood and normoxic tissues[57]. This allows for a shorter time interval between injection and imaging[58]. In addition, [^{18}F]FAZA has a high parent fraction during imaging, accounting for a parent fraction of 90% at 70 min after injection[59]. Other more hydrophilic nitroimidazole tracers include [^{18}F]FETNIM and [^{18}F]HX4, which have a partition coefficient (log P) of 0.17[60] and -0.69[61], respectively. An example of a more lipophilic tracer is [^{18}F]EF5, which is the ^{18}F-labelled version of exogenous hypoxia marker EF5, with a partition coefficient (log P) of 0.6.

Thiosemicarbazone-based tracers: Thiosemicarbazone-based tracers represent another subgroup of hypoxia tracers for PET. Thiosemicarbazones possess a strong antitumor activity, particularly when coupled with a metal ion like copper (Cu)[62]. [Cu]ATSM is a therapeutic agent which, by replacing the Cu atom with a suitable radioactive Cu isotope, can be used for hypoxia PET imaging[63]. In nuclear medicine, Cu is of particular interest for its favorable radiochemical properties. First, Cu is relatively easy to incorporate in molecules and has multiple radioactive isotopes suitable for PET imaging. Second, with half lives ranging from 24 min to 13h for ^{60}Cu and ^{64}Cu, respectively, Cu has several potential applications. The short-lived radionuclides can be used for sequential measurements, whereas radionuclides with longer half lives do

Table 1 Evaluated hypoxia tracers in oncology

Tracer[1]	Half-life	Validation studies[2,3]					Evaluated in clinical oncology[3]	
		BC	Probe	Ex-M	En-M	FMISO	Lung cancer	Other cancer types
[*Cu]ATSM	[60Cu]: 23.7 min [61Cu]: 3.3 h [62Cu]: 9.7 min [64Cu]: 12.7 h	Lewis *et al*[133], Yuan *et al*[134], Kersemans *et al*[135], Matsumoto *et al*[136]	Ballegeer *et al*[137], Bowen *et al*[138], Lewis *et al*[133], Myerson *et al*[139], O'Donoghue *et al*[72]	Ballegeer *et al*[137], Hansen *et al*[140], Matsumoto *et al*[136], McCall *et al*[66], O'Donoghue *et al*[72], Oh *et al*[74], Yuan *et al*[134]	Grigsby *et al*[141], Tateishi *et al*[142], Valtorta *et al*[143], Weeks *et al*[144]	Dence *et al*[145], Kersemans *et al*[135], Lewis *et al*[146], Matsumoto *et al*[136], O'Donoghue *et al*[72]	Dehdashti *et al*[86], Lohith *et al*[67], Wong *et al*[80], Zhang *et al*[81]	Chao *et al*[147], Dehdashti *et al*[148], Dehdashti *et al*[149], Dietz *et al*[150], Grassi *et al*[151], Grigsby *et al*[141], Kositwattanarerk *et al*[152], Laforest *et al*[153], Lewis *et al*[154], Minagawa *et al*[155], Nyflot *et al*[156]
[^{18}F]EF1	110 min	NA	NA	Evans *et al*[157]	NA	NA	NA	NA
[^{18}F]EF3		Mahy *et al*[158], Mahy *et al*[159]	NA	Mahy *et al*[159]	NA	Mahy *et al*[158], Dubois *et al*[160]	NA	Mahy *et al*[161]
[^{18}F]EF5		NA	NA	Yapp *et al*[162], Ziemer *et al*[163]	NA	NA	NA	Komar *et al*[164]
[^{18}F]FAZA [^{18}F]FETA		Reischl *et al*[165], Piert *et al*[166], Picchio *et al*[167], Maier *et al*[168], Tran *et al*[169] Barthel *et al*[187]	Busk *et al*[170], Mortensen *et al*[171], Piert *et al*[166], Tran *et al*[169] Barthel *et al*[187]	Busk *et al*[170], Busk *et al*[172], Busk *et al*[173], Busk *et al*[174], Busk *et al*[175], Graves *et al*[176], Maier *et al*[168], Solomon *et al*[177] NA	Belloli *et al*[178], Picchio *et al*[167], Troost *et al*[179], Valtorta *et al*[143] NA	Sorger *et al*[57], Piert *et al*[166], Reischl *et al*[165] Rasey *et al*[188]	Postema *et al*[180], Bollineni *et al*[181], Trinkaus *et al*[58], Verwer *et al*[59] NA	Grosu *et al*[182], Souvatzoglou *et al*[183], Schuetz *et al*[184], Shi *et al*[106], Mortensen *et al*[185], Havelund *et al*[186] NA
[^{18}F]FETNIM		Grönroos *et al*[189]	Yang *et al*[60]	NA	Hu *et al*[85]	Grönroos *et al*[189], Tolvanen *et al*[190], Yang *et al*[60]	Hu *et al*[85], Li *et al*[84]	Lehtiö *et al*[99], Lehtiö *et al*[191], Lehtiö *et al*[192], Vercellino *et al*[193], Yue *et al*[194]
[^{18}F]FMISO		Bentzen *et al*[195], Rasey *et al*[196], Bentzen *et al*[197], Troost *et al*[198]	Bentzen *et al*[125], Gagel *et al*[126], Bruehlmeier *et al*[199], Lawrentschuk *et al*[200], O'Donoghue *et al*[72], Piert *et al*[166], Sørensen *et al*[201], Gagel *et al*[202], Carlin *et al*[203], Chang *et al*[204], Mortensen *et al*[127]	Hatano *et al*[205], Huang *et al*[206], Huang *et al*[207], Oehler *et al*[208], Cho *et al*[209], Troost *et al*[210], Matsumoto *et al*[136], Troost *et al*[198], Dubois *et al*[211]	Dubois *et al*[211], Cherk *et al*[212], Riesterer *et al*[213], Lehmann *et al*[214], Chen *et al*[215], Campanile *et al*[216], Cheng *et al*[217], Sato *et al*[218], Norikane *et al*[219]		Cherk *et al*[212], Eschmann *et al*[77], Gagel *et al*[82], Koh *et al*[87], Rasey *et al*[220], Vera *et al*[83]	Koh *et al*[221], Liu *et al*[222], Yeh *et al*[223], Rischin *et al*[224], Bentzen *et al*[125], Rajendran *et al*[225], Gagel *et al*[126], Rajendran *et al*[226], Hicks *et al*[227], Lawrentschuk *et al*[200], Loi *et al*[228], Thorwarth *et al*[229], Rajendran *et al*[230], Rischin *et al*[231], Thorwarth *et al*[232], Zimny *et al*[124], Eschmann *et al*[233], Gagel *et al*[202], Thorwarth *et al*[234], Thorwarth *et al*[235], Lee *et al*[236], Lin *et al*[237], Nehmeh *et al*[238], Roels *et al*[239], Dirix *et al*[240], Lee *et al*[241], Mortensen *et al*[127], Wang *et al*[56], Abolmaali *et al*[242], Bowen *et al*[138], Eary *et al*[243], Kikuchi *et al*[244], Hugonnet *et al*[131], Yamane *et al*[245], Mammar *et al*[246], Zips *et al*[247], Cheng *et al*[217], Henriques de Figueiredo *et al*[248], Okamoto *et al*[249], Sato *et al*[218], Segard *et al*[250], Tachibana *et al*[251], Norikane *et al*[219]
[^{18}F]FRP170		NA	NA	NA	NA	NA	Kaneta *et al*[252]	NA
[^{18}F]FPIMO		NA	NA	Busk *et al*[174]	NA	NA	NA	NA
[^{18}F]HX4		Dubois *et al*[61]	NA	Dubois *et al*[61]	Chen *et al*[215]	Chen *et al*[215]	van Loon *et al*[253], Zegers *et al*[78]	Chen *et al*[215]
[^{124}I]IAZA	4.2 d	Reischl *et al*[165]	NA	NA	NA	Reischl *et al*[165]	NA	NA
[^{124}I]IAZG		NA	Zanzonico *et al*[254]	NA	NA	Riedl *et al*[255], Zanzonico *et al*[254]	NA	NA

[1]Refer to Table 2 for full tracer names; [2]Preclinical and clinical studies comparing the uptake of the hypoxia tracer under study with other hypoxia markers; [3]Excluding brain studies. BC: Induced hypoxia by breathing conditions; Probe: Polarograpic electrode; Ex-M: Exogenous hypoxia marker (pimonidazole, EF3 or EF5); En-M: Endogenous hypoxia marker (HIF-1, CA IX); FMISO: [18F]FMISO PET; NA: Not available.

Table 2 Hypoxia positron emission tomography tracer abbreviations

Abbreviation	Full name or chemical name
[*Cu]ATSM	[*Cu]-diacetyl-bis(N4-methylthiosemicarbazone)
[^{18}F]EF1	2-(2-Nitroimidazol-1H-yl)-N-(3-[^{18}F]fluoropropyl)acetamide
[^{18}F]EF3	2-(2-Nitroimidazol-1H-yl)-N-(3,3,3-[^{18}F]trifluoropropyl)acetamide
[^{18}F]EF5	2-(2-nitro-1H-imidazol-1-yl)-N-(2,2,3,3,3-[^{18}F]-pentafluoropropyl)-acetamide
[^{18}F]FAZA	[^{18}F]fluoroazomycin arabinoside
[^{18}F]FETA	[^{18}F]fluoroetanidazole
[^{18}F]FETNIM	[^{18}F]fluoroerythronitroimidazole
[^{18}F]FMISO	[^{18}F]fluoromisonidazole
[^{18}F]FRP170	1-(2-[^{18}F]fluoro-1-[hydroxymethyl]ethoxy)methyl-2-nitroimidazole
[^{18}F]FPIMO	[^{18}F]pimonidazole
[^{18}F]HX4	3-[^{18}F]fluoro-2-(4-((2-nitro-1H-imidazol-1-yl)methyl)-1H-1,2,3,-triazol-1-yl)-propan-1-ol
[^{124}I]IAZA	[^{124}I]iodazomycin arabinoside
[^{124}I]IAZG	[^{124}I]iodazomycin galactoside

not require a cyclotron on-site and are more suitable for the clinical setting. Remarkably, ^{64}Cu can also be applied as radiation therapy agent, since it also emits a β^- particle (40% yield)[64,65]. In oncology, [Cu]ATSM has been evaluated both preclinically and clinically. This tracer shows favorable kinetics with rapid uptake in hypoxic tissue and fast clearance from normoxic tissues, enabling imaging within 30 min after injection[66,67]. However, the exact uptake mechanism of [Cu]ATSM is still under debate[63,68,69] and several preclinical studies have shown that [Cu]ATSM uptake depends on tumor type and other characteristics than hypoxia alone[70-76].

Clinical evaluation of hypoxia PET tracers in lung cancer

Hypoxia PET imaging is in development and most clinical studies have been focused on notoriously hypoxic cancer types such as cervical cancer and head and neck cancer. Nevertheless, several clinical PET studies have evaluated hypoxia imaging in lung cancer (Table 3). In the following paragraphs, data acquisition, quantification and clinical observations of these hypoxia tracers will be discussed.

Data acquisition and analysis: Nitroimidazole based tracers require relatively long time intervals for accumulation in hypoxic cells and clearance from normoxic cells. In concordance, most studies used images > 2 h after injection for hypoxia assessment. The length of the time interval between injection and imaging may affect the tracers' distribution pattern in tumors. For example, it has been shown that the distribution of [^{18}F]FMISO at 2 h is significantly different from the distribution at 4 h, whereas only the 4 h data are predictive of tumor recurrence[77]. In contrast, the distribution of [^{18}F]HX4 was similar at 2 h and 4 h[78]. Compared to nitroimidazole based tracers, [Cu]ATSM shows fast kinetics and images were acquired after time intervals as short as 10 min after injection[67,79-81].

Quantification of hypoxia: To identify hypoxia in tumor tissue, several simplified parameters have been used, including tumor-to-blood ratio, tumor-to-background ratio, tumor-to-muscle ratio, tumor-to-mediastinum ratio, and SUV. In addition, several studies have used dynamic PET scans to investigate the tracers' kinetics in more detail, for example by using pharmacokinetic modeling for quantification[59]. Furthermore, consecutive imaging using multiple tracers has been performed to facilitate the identification and quantification of hypoxia. For example, consecutive PET scans have been performed with hypoxia tracer [Cu]ATSM and perfusion tracer copper-pyruvaldehyde-bis(N4-methylthiosemicarbazone ([Cu]PTSM). Here, the ratio of [Cu]ATSM SUV to [Cu]PTSM SUV has been used as a measure of hypoxia[81].

To date, it is not known which measure and threshold accurately reflects pO_2 levels in tumors. As repeated measurements with a polarographic electrode are not feasible in lung cancer, a more pragmatic approach is required. The clinical relevance of a threshold can be determined by clinical parameters like tumor response, progression-free survival and overall survival.

Determination of clinically relevant hypoxia: Among the clinical studies on hypoxia PET tracers in lung cancer, most studies have only evaluated tumor hypoxia prior to treatment. For [^{18}F]FMISO, a pretreatment threshold of > 2 for tumor-to-mediastinum ratio was associated with poor outcome after radiation therapy. However, the shape of the time activity curve appeared to be a better predictor of response[77]. In contrast to these results, other authors did not find a predictive value for [^{18}F]FMISO after chemoradiation[82,83]. In other patients treated with chemoradiation, a threshold of tumor-to-blood ratio > 1.9 for [^{18}F]FETNIM[84,85] and > 3.0 for [Cu]ATSM[86] was associated with poor overall survival and tumor response, respectively. In addition, a number of studies have evaluated the changes in hypoxia tracer uptake during therapy. While hypoxic cells are considered to be more resistant to radiation therapy, most studies in lung cancer reported a decrease in hypoxia tracer uptake after radiation therapy[58,82,87].

PET FOR TUMOR PERFUSION MEASUREMENTS

Tumor angiogenesis

Blood flow is not only required for the delivery of PET tracers and anticancer drugs to tumors, but also for the

Table 3 Hypoxia tracer studies in lung cancer

Tracer[1]	Year	Authors	N[2]	Stage	Time[3]	Duration[4]	Measure[5]	Therapy[6]
[^{60}Cu]ATSM	2003	Dehdashti *et al*[86]	18	I -IV	30 min	30 min	T/M	Radiation Chemoradiation, chemotherapy
[^{62}Cu]ATSM	2000	Takahashi *et al*[79]	6	NA	10 min	10 min	T/B	
	2008	Wong *et al*[80]	2	NA	15 min	5 min	SUV	
	2009	Lohith *et al*[67]	13	I -IV	10 min	10 min	SUV_{mean}	
	2013	Zhang *et al*[81]	5	I -IV	15 min	5 min	$SUV_{hypoxia/perfusion}$ [7]	
[^{18}F]FAZA	2009	Postema *et al*[180]	13	NA	2-3 h	3-4 min	T/Bg	
	2013	Trinkaus *et al*[58]	11	III	4 h	30 min	T/Bg	Chemoradiation
	2013	Bollineni *et al*[181]	11	III-IV	2 h	NA	T/Bg	
	2013	Verwer *et al*[59]	9	NA	0 h	70 min[8]	V_T[9]	
[^{18}F]FETNIM	2010	Li *et al*[84]	26	III	2 h	20 min	T/B_{max}	Radiation Chemotherapy
	2013	Hu *et al*[85]	25	II	2 h	NA	T/Me	Chemotherapy
[^{18}F]FMISO	1995	Koh *et al*[87]	14	III	2 h	40 min	T/B	Radiation
	1996	Rasey *et al*[220]	21	III-IV	2 h	40 min	T/B	
	2005	Eschmann *et al*[77]	8	III-IV	4 h	NA	T/Me	Radiation
	2006	Cherk *et al*[212]	21	I - II	2 h	NA	SUV_{max}	
	2006	Gagel *et al*[82]	8	III-IV	3 h	30 min	SUV, T/M	Chemoradiation
	2011	Vera *et al*[83]	7	III	3 h	NA	SUV_{max}	Chemoradiation Chemotherapy
[^{18}F]FRP170	2007	Kaneta *et al*[252]	3	NA	0 h	60 min[8]	SUV TAC	
[^{18}F]HX4	2010	van Loon *et al*[253]	4	IV	2 h	NA	T/B	
	2013	Zegers *et al*[78]	15	II -IV	4 h	30 min	T/B	

[1]Refer to Table 2 for full tracer names; [2]Number of lung cancer patients (evaluable scans); [3]Start time after injection of the positron emission tomography (PET) frame that was used for quantification; [4]Duration of the PET frame that was used for quantification; [5](Semi)quantitative measure used for evaluation; [6]Evaluated therapy; [7]Hypoxia marker uptake normalized to perfusion marker uptake: mean (SUV[Cu]ATSM/SUV[Cu]PTSM); [8]Dynamic PET data used for quantification; [9]Volume of distribution derived from full pharmacokinetic modeling. NA: Data not available; SUV: Standardized uptake value; T/M: Tumor-to muscle ratio; T/Me: Tumor-to-mediastinum ratio; T/B: Tumor-to-blood ratio; T/Bg: Tumor-to-background ratio; VT: Volume of distribution; TAC: Time activity curve.

transport of nutrients, *e.g.*, glucose, and oxygen. Under hypoxic conditions in tumors, the HIF protein is usually upregulated. Activated HIF translocates to the nucleus of tumor cells and results in transcription of a large repertoire of genes including VEGF[88,89]. VEGF is a potent protein and plays a key role in tumor angiogenesis, which is the formation of new blood vessels. This tumor angiogenesis is essential for tumor growth, metastatic spread and survival of tumor cells. As a result, VEGF signaling has become an important therapeutic target for the treatment of malignant tumors. To date, several antiangiogenic drugs have been developed including monoclonal antibodies that bind circulating VEGF (*e.g.*, bevacizumab[90]) and tyrosine kinase inhibitors that target the intracellular domain of the VEGF receptors (*e.g.*, sunitinib and sorafenib[91]). Among the currently available antiangiogenic drugs, bevacizumab has been registered for the treatment of patients with NSCLC. In combination with paclitaxel and carboplatin, bevacizumab has been approved for first-line treatment of non-squamous NSCLC[15]. As tumor vascularization is an important factor in the biology of malignant tumors, and antiangiogenic strategies have been introduced for the treatment of lung cancer, imaging techniques are increasingly used for perfusion measurements in lung cancer.

Imaging of tumor perfusion

PET is a sensitive technique to quantify tumor perfusion[92]. To this end, perfusion tracers like rubidium-82 (^{82}Rb[93]), radioactive ammonia ([^{13}N]NH_3[94]), radioactive water ([^{15}O]H_2O[95-101]) can be administered. Other PET tracers such as [^{68}Ga]transferrin[102] and [^{11}C]methylalbumin[103] are available to assess vascular permeability. Currently, experience with perfusion PET tracers is rather limited in oncology, except for [^{15}O]H_2O. In particular, previous PET studies have shown that quantification of tumor perfusion using [^{15}O]H_2O is feasible in patients with lung cancer [97,104,105].

[^{15}O]H_2O PET

As [^{15}O]H_2O is a freely diffusible tracer with near 100% extraction over a wide perfusion range (0-6 mL/min per mL), its kinetics directly reflect tumor perfusion. As a result, [^{15}O]H_2O is an ideal tracer for quantitative perfusion imaging. The short half-life of ^{15}O, which is 2.03 min, enables sequential PET scans using both [^{15}O]H_2O and another tracer, *e.g.*, [^{18}F]FDG[97] or a hypoxia tracer[106]. However, it requires the presence of a nearby cyclotron. Because [^{15}O]H_2O is metabolically inert and is not retained in cells, quantification using SUV, which is a parameter for quantification of irreversible uptake, is not

possible. Instead, pharmacokinetic modeling, using short (< 10 min) dynamic PET scans, is required to quantify tumor perfusion.

Monitoring tumor perfusion during treatment

Currently, [^{15}O]H_2O PET scans are increasingly used to assess response of the tumor vasculature to antiangiogenic therapy[107-110]. As [^{15}O]H_2O PET has shown high reproducibility in lung cancer[105], it can be applied for response monitoring during treatment. de Langen *et al*[111] have investigated changes in tumor perfusion in 44 NSCLC patients who were treated with bevacizumab and erlotinib. Three weeks after the start of treatment, a mean decrease of 11% in tumor perfusion was measured using [^{15}O]H_2O PET[111]. A significant reduction in tumor perfusion was measured in patients with a partial response according to the response evaluation criteria in solid tumors (RECIST[112]). More importantly, patients with > 20% reduction in tumor perfusion had an improved progression-free survival as compared to other patients (12.5 mo *vs* 2.9 mo). The latter findings indicate that [^{15}O]H_2O PET may have predictive value in lung cancer patients who are treated with antiangiogenic drugs. For early prediction of tumor response, early perfusion measurements may be useful, as the effects of antiangiogenic can be very rapid[113].

Tumor perfusion and drug delivery

As the short half-life of ^{15}O enables sequential PET scans using both [^{15}O]H_2O and an additional tracer, [^{15}O]H_2O PET is a useful tool to investigate drug delivery of radiolabeled anticancer agents by correlating uptake of radiolabeled drugs with [^{15}O]H_2O perfusion data[114,115]. Apparently, it has been shown that tumor perfusion is an important determinant of drug tumor exposure, as indicated by several PET studies on [^{18}F]5-fluorouracil(FU)[116-118], [^{11}C]DACA[119], and [^{11}C]docetaxel[120,121]. Consequently, tumor perfusion may be predictive of tumor response to the above mentioned anticancer drugs. These findings advocate further studies investigating the predictive value of tumor perfusion for tumor response to chemotherapy. As tumor perfusion is the key factor for the uptake of several anticancer drugs in tumors[122], antiangiogenic drugs may affect drug exposure in tumors. To investigate this concept, a PET study has been performed in NSCLC patients using both [^{15}O]H_2O and the radiolabeled taxane [^{11}C]docetaxel[113]. In that study, bevacizumab reduced both perfusion and net influx rate of [^{11}C]docetaxel within 5 h. These rapid effects persisted after 4 d and were not associated with significant changes in tumor heterogeneity. The mentioned studies indicate that [^{15}O]H_2O PET may reveal the role of perfusion in drug delivery and antiangiogenic therapy in malignant tumors[123].

IMAGING HYPOXIA AND PERFUSION

It is conceivable that the development of tumor hypoxia is associated with a decrease in tumor perfusion. This may complicate PET imaging, as tracer delivery will be reduced in these areas. Although the uptake of the ideal hypoxia tracer is not directly related to perfusion, lack of perfusion will limit tracer delivery.

Diffusion-limited hypoxia is present in tumor cells located away from capillaries, *i.e.*, further than the diffusion distance of oxygen. As perfusion is relatively low in these areas, tracer delivery may be limited and this may, in turn, affect uptake of hypoxia tracers. In addition, low perfused areas can become necrotic. The PET signal will be decreased in areas containing necrosis even though these areas may also contain highly hypoxic cells. In Figure 4, these hypothetical considerations are summarized. The figure also illustrates the limitations of using a predefined threshold to delineate hypoxic areas on a PET image, as areas likely to contain the most severely hypoxic cells will be missed. The mentioned considerations may explain the conflicting results between the uptake of hypoxia tracers and the direct assessment of tissue oxygenation using polarographic electrodes[124-127]. [^{15}O]H_2O PET may help to understand these conflicting results and may identify the remote, low perfused areas. An example of images obtained from consecutive perfusion and hypoxia PET imaging is displayed in Figure 5.

Acute hypoxia is directly caused by a (temporary) lack of tumor perfusion. Since acute hypoxia is presumed to be transient or even cycling[128], hypoxia tracer uptake may not accurately reflect this type of hypoxia. [^{15}O]H_2O PET may help to study the effect of acute hypoxia and its relation with hypoxia tracer uptake.

Besides the previous considerations for combining [^{15}O]H_2O perfusion PET imaging with hypoxia tracer PET imaging, the combination may provide further insight into the effects of treatment. Jain has previously proposed that antiangiogenic therapy may normalize the abnormal tumor vasculature, thereby decreasing tumor hypoxia and improving drug delivery of cytotoxic agents[129,130]. This is underscored by the fact that a decrease in [^{18}F]FMISO uptake has been measured in renal cell cancer after treatment with sunitinib[131]. On the other hand, an increase in [^{18}F]FMISO uptake after sorafenib[132] and a rapid decrease in tumor perfusion after bevacizumab have been reported as well[113]. The latter findings suggest that antiangiogenic therapy may decrease tumor perfusion and subsequently the delivery of hypoxia tracers to tumors. To further clarify these findings, future PET studies need to combine hypoxia tracers with [^{15}O]H_2O at different time points after drug administration.

FUTURE PERSPECTIVES

In the present review, the currently available tracers for PET imaging of hypoxia and perfusion in lung cancer patients were discussed. Considering the currently available studies, PET seems feasible to assess hypoxia and perfusion in lung cancer. In contrast to traditional probe measurements, PET hypoxia imaging is non-invasive and provides information on the heterogeneous distribution

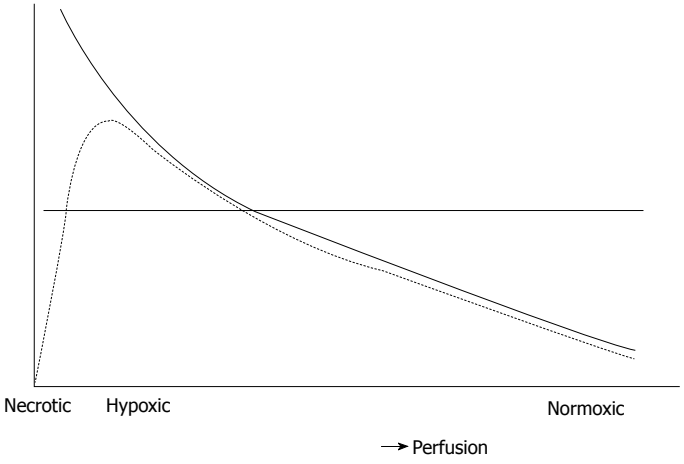

Figure 4 Representation of hypothetical considerations on the link between perfusion and the hypoxia signal as measured by imaging positron emission tomography. The continuous curve represents hypothetical level of hypoxia in tissue for increasing levels of perfusion (*i.e.*, closer to the capillaries). The dotted line represents the positron emission tomography signal obtained from hypoxia imaging using an optimal imaging protocol. The horizontal line represents a threshold used for delineation of hypoxic areas.

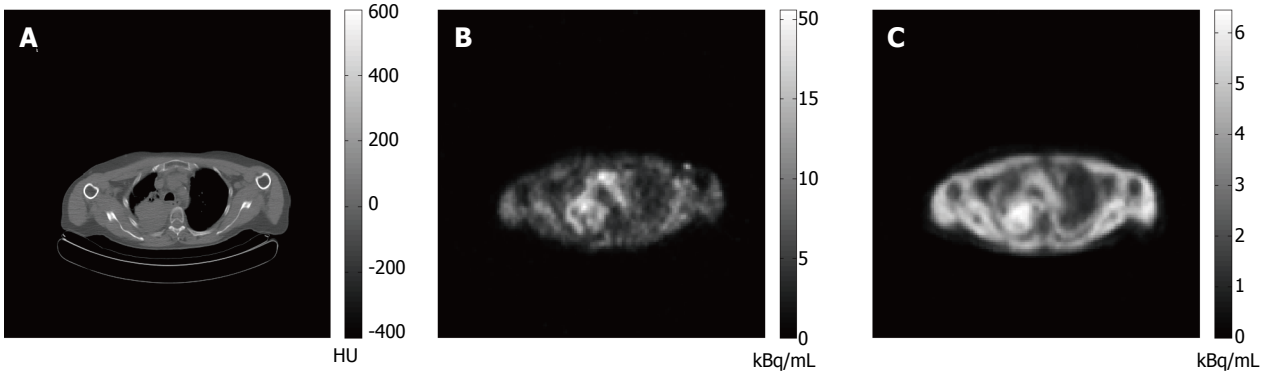

Figure 5 Example of consecutive perfusion and hypoxia positron emission tomography in a patient with non-small cell lung cancer. A: Low dose computed tomography; B: Perfusion image (averaged image acquired over time interval 30-120 s after injection of 370 MBq [^{15}O]H_2O); C: Hypoxia image (averaged image over time interval 40-70 min after injection of 185 MBq [^{18}F]FAZA).

of hypoxia in tumors. In addition, whole body PET scans using a hypoxia tracer can reveal hypoxic areas not only in primary tumors, but in metastases as well. To date, several tracers have been developed to measure tumor hypoxia, whereas tumor perfusion has been mostly quantified using [^{15}O]H_2O. While acquisition and quantification of [^{15}O]H_2O data is rather straightforward, several challenges remain for PET hypoxia tracers.

Although several hypoxia tracers have been developed and evaluated in the clinical setting, no consensus has yet been reached on the most feasible tracer, the optimal timing of acquisition, and the most accurate quantification method. In lung cancer, the studies on hypoxia PET tracers are preliminary and include a limited number of patients. Ideally, the clinical impact of hypoxia imaging would be evaluated in large clinical trials validating hypoxia tracers for prediction of tumor response and survival. In addition, clinical trials are needed to reveal the clinical value of hypoxia tracers for advanced radiation therapy strategies such as dose painting. In NSCLC, several trials are currently recruiting patients for [^{18}F]FMISO based (NCT01576796) and [^{18}F]FDG based (NCT01024829) dose boosting.

In patients with lung cancer, quantification of tracer uptake can be challenging due to tumor movement during respiration. As PET acquisition usually takes 10min to 1 h, patient motion during PET imaging is unavoidable and the acquired image of the lung tumor will be blurred, which complicates accurate delineation of hypoxic areas. As a result, these images are less suitable for dose painting techniques, especially for dose painting by numbers. For PET imaging, respiratory gated imaging (4D imaging) is currently under study. In respiratory gated imaging, patient motion is continuously monitored during acquisition. As a result, PET data can either be corrected for the registered motion or PET data from a specific interval of the respiratory cycle can be used for reconstruction. As similar techniques are also under study for radiation therapy, dose painting strategies may be further improved by combining 4D PET hypoxia imaging with 4D radiation therapy.

Since the introduction of antiangiogenic drugs, perfusion measurements have been increasingly applied in the clinic. [^{15}O]H_2O PET provides quantification of tumor perfusion and may be useful for response monitoring during antiangiogenic therapy. Further studies are needed to evaluate the predictive value of tumor perfusion for tumor response to anti-cancer drugs. In addition, tumor perfusion may not only affect the delivery of drugs to tumors, but also the delivery of PET tracers such as hypoxia tracers.

In conclusion, PET using both [^{15}O]H_2O and a hy-

poxia tracer is a promising method to further understand the development of hypoxia in lung cancer. As previously mentioned, these PET scans are promising for response monitoring of radiation therapy and antiangiogenic drugs. In addition, hypoxia tracers may be useful to select patients for treatment with radiosensitizers (*e.g.*, nimorazole, NCT01733823) and realize a more precise radiation plan including dose boosting and dose painting. As the available PET studies on hypoxia and perfusion are rather preliminary in patients with lung cancer, further studies are needed for validation and clinical implementation in this patient population.

ACKNOWLEDGMENTS

This review was written within the framework of CTMM, the Center for Translational Molecular Medicine.

REFERENCES

1 **Jemal A**, Siegel R, Xu J, Ward E. Cancer statistics, 2010. *CA Cancer J Clin* 2010; **60**: 277-300 [PMID: 20610543 DOI: 10.1200/JCO.2003.11.132]
2 **Jemal A**, Siegel R, Ward E, Murray T, Xu J, Thun MJ. Cancer statistics, 2007. *CA Cancer J Clin* 2007; **57**: 43-66 [PMID: 17237035 DOI: 10.3322/canjclin.57.1.43]
3 **Brambilla E**, Travis WD, Colby TV, Corrin B, Shimosato Y. The new World Health Organization classification of lung tumours. *Eur Respir J* 2001; **18**: 1059-1068 [PMID: 11829087 DOI: 10.1183/09031936.01.00275301]
4 **DeVita VTHS**, Rosenberg SA. Principles and practice of oncology. USA: Lippincott Williams & Wilkins, 2008
5 **Mountain CF**. Revisions in the International System for Staging Lung Cancer. *Chest* 1997; **111**: 1710-1717 [PMID: 9187198 DOI: 10.1378/chest.111.6.1710]
6 **Rosti G**, Bevilacqua G, Bidoli P, Portalone L, Santo A, Genestreti G. Small cell lung cancer. *Ann Oncol* 2006; **17** (suppl 2): ii5-ii10 [DOI: 10.1093/annonc/mdj910]
7 **Goffin J**, Lacchetti C, Ellis PM, Ung YC, Evans WK. First-line systemic chemotherapy in the treatment of advanced non-small cell lung cancer: a systematic review. *J Thorac Oncol* 2010; **5**: 260-274 [PMID: 20101151 DOI: 10.1097/JTO.0b013e3181c6f035]
8 **Grossi F**, Kubota K, Cappuzzo F, de Marinis F, Gridelli C, Aita M, Douillard JY. Future scenarios for the treatment of advanced non-small cell lung cancer: focus on taxane-containing regimens. *Oncologist* 2010; **15**: 1102-1112 [PMID: 20930102 DOI: 10.1634/theoncologist.2010-0322]
9 **Shepherd FA**, Rodrigues Pereira J, Ciuleanu T, Tan EH, Hirsh V, Thongprasert S, Campos D, Maoleekoonpiroj S, Smylie M, Martins R, van Kooten M, Dediu M, Findlay B, Tu D, Johnston D, Bezjak A, Clark G, Santabárbara P, Seymour L. Erlotinib in previously treated non-small-cell lung cancer. *N Engl J Med* 2005; **353**: 123-132 [PMID: 16014882 DOI: 10.1056/NEJMoa050753]
10 **Cappuzzo F**, Ciuleanu T, Stelmakh L, Cicenas S, Szczésna A, Juhász Eb, Esteban E, Molinier O, Brugger W, Melezínek I, Klingelschmitt Gl, Klughammer B, Giaccone G. Erlotinib as maintenance treatment in advanced non-small-cell lung cancer: a multicentre, randomised, placebo-controlled phase 3 study. *The Lancet Oncol* 2010; **11**: 521-529 [DOI: 10.1016/S1470-2045(10)70112-1]
11 **Cohen MH**, Williams GA, Sridhara R, Chen G, McGuinn WD, Morse D, Abraham S, Rahman A, Liang C, Lostritto R, Baird A, Pazdur R. United States Food and Drug Administration Drug Approval summary: Gefitinib (ZD1839; Iressa) tablets. *Clin Cancer Res* 2004; **10**: 1212-1218 [PMID: 14977817 DOI: 10.1158/1078-0432.CCR-03-0564]
12 **Tsao MS**, Sakurada A, Cutz JC, Zhu CQ, Kamel-Reid S, Squire J, Lorimer I, Zhang T, Liu N, Daneshmand M, Marrano P, da Cunha Santos G, Lagarde A, Richardson F, Seymour L, Whitehead M, Ding K, Pater J, Shepherd FA. Erlotinib in lung cancer - molecular and clinical predictors of outcome. *N Engl J Med* 2005; **353**: 133-144 [PMID: 16014883 DOI: 10.1056/NEJMoa050736]
13 **Paez JG**, Jänne PA, Lee JC, Tracy S, Greulich H, Gabriel S, Herman P, Kaye FJ, Lindeman N, Boggon TJ, Naoki K, Sasaki H, Fujii Y, Eck MJ, Sellers WR, Johnson BE, Meyerson M. EGFR mutations in lung cancer: correlation with clinical response to gefitinib therapy. *Science* 2004; **304**: 1497-1500 [PMID: 15118125 DOI: 10.1126/science.1099314]
14 **Lynch TJ**, Bell DW, Sordella R, Gurubhagavatula S, Okimoto RA, Brannigan BW, Harris PL, Haserlat SM, Supko JG, Haluska FG, Louis DN, Christiani DC, Settleman J, Haber DA. Activating mutations in the epidermal growth factor receptor underlying responsiveness of non-small-cell lung cancer to gefitinib. *N Engl J Med* 2004; **350**: 2129-2139 [PMID: 15118073 DOI: 10.1056/NEJMoa040938]
15 **Sandler A**, Gray R, Perry MC, Brahmer J, Schiller JH, Dowlati A, Lilenbaum R, Johnson DH. Paclitaxel-carboplatin alone or with bevacizumab for non-small-cell lung cancer. *N Engl J Med* 2006; **355**: 2542-2550 [PMID: 17167137 DOI: 10.1056/NEJMoa061884]
16 **Shaw AT**, Kim DW, Nakagawa K, Seto T, Crinó L, Ahn MJ, De Pas T, Besse B, Solomon BJ, Blackhall F, Wu YL, Thomas M, O'Byrne KJ, Moro-Sibilot D, Camidge DR, Mok T, Hirsh V, Riely GJ, Iyer S, Tassell V, Polli A, Wilner KD, Jänne PA. Crizotinib versus chemotherapy in advanced ALK-positive lung cancer. *N Engl J Med* 2013; **368**: 2385-2394 [PMID: 23724913 DOI: 10.1056/NEJMoa1214886]
17 **Le QT**, Chen E, Salim A, Cao H, Kong CS, Whyte R, Donington J, Cannon W, Wakelee H, Tibshirani R, Mitchell JD, Richardson D, O'Byrne KJ, Koong AC, Giaccia AJ. An evaluation of tumor oxygenation and gene expression in patients with early stage non-small cell lung cancers. *Clin Cancer Res* 2006; **12**: 1507-1514 [PMID: 16533775 DOI: 10.1158/1078-0432.CCR-05-2049]
18 **Koukourakis MI**, Giatromanolaki A, Sivridis E, Bougioukas G, Didilis V, Gatter KC, Harris AL. Lactate dehydrogenase-5 (LDH-5) overexpression in non-small-cell lung cancer tissues is linked to tumour hypoxia, angiogenic factor production and poor prognosis. *Br J Cancer* 2003; **89**: 877-885 [PMID: 12942121 DOI: 10.1038/sj.bjc.6601205]
19 **Giatromanolaki A**, Koukourakis MI, Sivridis E, Turley H, Talks K, Pezzella F, Gatter KC, Harris AL. Relation of hypoxia inducible factor 1 alpha and 2 alpha in operable non-small cell lung cancer to angiogenic/molecular profile of tumours and survival. *Br J Cancer* 2001; **85**: 881-890 [PMID: 11556841 DOI: 10.1054/bjoc.2001.2018]
20 **Swinson DEB,** Jones JL, Richardson D, Wykoff C, Turley H, Pastorek J, Taub N, Harris AL, O'Byrne KJ. Carbonic anhydrase IX expression, a novel surrogate marker of tumor hypoxia, is associated with a poor prognosis in non-small cell lung cancer. *J Clin Oncol* 2003; **21**: 473-482
21 **Harrison LB**, Chadha M, Hill RJ, Hu K, Shasha D. Impact of tumor hypoxia and anemia on radiation therapy outcomes. *Oncologist* 2002; **7**: 492-508 [PMID: 12490737 DOI: 10.1634/theoncologist.7-6-492]
22 **Song X**, Liu X, Chi W, Liu Y, Wei L, Wang X, Yu J. Hypoxia-induced resistance to cisplatin and doxorubicin in non-small cell lung cancer is inhibited by silencing of HIF-1alpha gene. *Cancer Chemother Pharmacol* 2006; **58**: 776-784 [PMID: 16532342 DOI: 10.1007/s00280-006-0224-7]
23 **Vaupel P**, Mayer A. Hypoxia in cancer: significance and impact on clinical outcome. *Cancer Metastasis Rev* 2007; **26**:

225-239 [PMID: 17440684 DOI: 10.1007/s10555-007-9055-1]
24 **Jain RK**. Normalizing tumor vasculature with anti-angiogenic therapy: a new paradigm for combination therapy. *Nat Med* 2001; **7**: 987-989 [PMID: 11533692 DOI: 10.1038/nm0901-987]
25 **Harris AL**. Hypoxia--a key regulatory factor in tumour growth. *Nat Rev Cancer* 2002; **2**: 38-47 [PMID: 11902584 DOI: 10.1038/nrc704]
26 **Kim SJ**, Rabbani ZN, Dewhirst MW, Vujaskovic Z, Vollmer RT, Schreiber EG, Oosterwijk E, Kelley MJ. Expression of HIF-1alpha, CA IX, VEGF, and MMP-9 in surgically resected non-small cell lung cancer. *Lung Cancer* 2005; **49**: 325-335 [PMID: 15935515 DOI: 10.1016/j.lungcan.2005.03.036]
27 **Younes M,** Brown RW, Stephenson M, Gondo M, Cagle PT. Overexpression of Glut1 and Glut3 in stage I nonsmall cell lung carcinoma is associated with poor survival. *Cancer* 1997; **80**: 1046-1051 [DOI: 10.1002/(SICI)1097-0142(19970915)80: 6<1046: : AID-CNCR6>3.0.CO; 2-7]
28 **Le QT**, Courter D. Clinical biomarkers for hypoxia targeting. *Cancer Metastasis Rev* 2008; **27**: 351-362 [PMID: 18483785 DOI: 10.1007/s10555-008-9144-9]
29 **Hockel M**, Schlenger K, Aral B, Mitze M, Schaffer U, Vaupel P. Association between tumor hypoxia and malignant progression in advanced cancer of the uterine cervix. *Cancer Res* 1996; **56**: 4509-4515 [PMID: 8813149]
30 **Carlin S**, Humm JL. PET of hypoxia: current and future perspectives. *J Nucl Med* 2012; **53**: 1171-1174 [PMID: 22789676 DOI: 10.2967/jnumed.111.099770]
31 **Brown JM**, Wilson WR. Exploiting tumour hypoxia in cancer treatment. *Nat Rev Cancer* 2004; **4**: 437-447 [PMID: 15170446 DOI: 10.1038/nrc1367]
32 **Wilson WR**, Hay MP. Targeting hypoxia in cancer therapy. *Nat Rev Cancer* 2011; **11**: 393-410 [PMID: 21606941 DOI: 10.1038/nrc3064]
33 **Boellaard R.** Standards for PET image acquisition and quantitative data analysis. *J Nucl Med* 2009; **50** Suppl 1: 11S-20S
34 **Gunn RN**, Gunn SR, Cunningham VJ. Positron emission tomography compartmental models. *J Cereb Blood Flow Metab* 2001; **21**: 635-652 [PMID: 11488533 DOI: 10.1097/00004647-200106000-00002]
35 **Lardinois D**, Weder W, Hany TF, Kamel EM, Korom S, Seifert B, von Schulthess GK, Steinert HC. Staging of non-small-cell lung cancer with integrated positron-emission tomography and computed tomography. *N Engl J Med* 2003; **348**: 2500-2507 [PMID: 12815135 DOI: 10.1056/NEJMoa022136]
36 **van Tinteren TH**, Hoekstra OS, Smit EF, van den Bergh JH, Schreurs AJ, Stallaert RA, van Velthoven PC, Comans EF, Diepenhorst FW, Verboom P, van Mourik JC, Postmus PE, Boers M, Teule GJ. Effectiveness of positron emission tomography in the preoperative assessment of patients with suspected non-small-cell lung cancer: the PLUS multicentre randomised trial. *Lancet* 2002; **359**: 1388-1393 [DOI: 10.1016/S0140-6736(02)08352-6]
37 **Pieterman RM**, van Putten JW, Meuzelaar JJ, Mooyaart EL, Vaalburg W, Koëter GH, Fidler V, Pruim J, Groen HJ. Preoperative staging of non-small-cell lung cancer with positron-emission tomography. *N Engl J Med* 2000; **343**: 254-261 [PMID: 10911007 DOI: 10.1056/NEJM200007273430404]
38 **Dierckx RA**, Van de Wiele C. FDG uptake, a surrogate of tumour hypoxia? *Eur J Nucl Med Mol Imaging* 2008; **35**: 1544-1549 [PMID: 18509637 DOI: 10.1007/s00259-008-0758-5]
39 **Gray LH**, Conger AD, Ebert M, Hornsey S, Scott OC. The concentration of oxygen dissolved in tissues at the time of irradiation as a factor in radiotherapy. *Br J Radiol* 1953; **26**: 638-648 [PMID: 13106296 DOI: 10.1259/0007-1285-26-312-638]
40 **Chapman JD**, Dugle DL, Reuvers AP, Meeker BE, Borsa J. Letter: Studies on the radiosensitizing effect of oxygen in Chinese hamster cells. *Int J Radiat Biol Relat Stud Phys Chem Med* 1974; **26**: 383-389 [PMID: 4548052 DOI: 10.1080/09553007414551361]
41 **Teicher BA**. Hypoxia and drug resistance. *Cancer Metastasis Rev* 1994; **13**: 139-168 [PMID: 7923547 DOI: 10.1007/BF00689633]
42 **Trédan O**, Galmarini CM, Patel K, Tannock IF. Drug resistance and the solid tumor microenvironment. *J Natl Cancer Inst* 2007; **99**: 1441-1454 [PMID: 17895480 DOI: 10.1093/jnci/djm135]
43 **Semenza GL**. Targeting HIF-1 for cancer therapy. *Nat Rev Cancer* 2003; **3**: 721-732 [PMID: 13130303 DOI: 10.1038/nrc1187]
44 **Hu Y**, Liu J, Huang H. Recent agents targeting HIF-1α for cancer therapy. *J Cell Biochem* 2013; **114**: 498-509 [PMID: 22961911 DOI: 10.1002/jcb.24390]
45 **von Pawel J**, von Roemeling R, Gatzemeier U, Boyer M, Elisson LO, Clark P, Talbot D, Rey A, Butler TW, Hirsh V, Olver I, Bergman B, Ayoub J, Richardson G, Dunlop D, Arcenas A, Vescio R, Viallet J, Treat J. Tirapazamine plus cisplatin versus cisplatin in advanced non-small-cell lung cancer: A report of the international CATAPULT I study group. Cisplatin and Tirapazamine in Subjects with Advanced Previously Untreated Non-Small-Cell Lung Tumors. *J Clin Oncol* 2000; **18**: 1351-1359 [PMID: 10715308]
46 **Henk JM**, Kunkler PB, Smith CW. Radiotherapy and hyperbaric oxygen in head and neck cancer. Final report of first controlled clinical trial. *Lancet* 1977; **2**: 101-103 [DOI: 10.1016/S0140-6736(77)90116-7]
47 **Kaanders JH**, Bussink J, van der Kogel AJ. ARCON: a novel biology-based approach in radiotherapy. *Lancet Oncol* 2002; **3**: 728-737 [DOI: 10.1016/S1470-2045(02)00929-4]
48 **Fyles AW,** Milosevic M, Pintilie M, Syed A, Hill RP. Anemia, hypoxia and transfusion in patients with cervix cancer: a review. *Radiother Oncol* 2000; **57**: 13-19 [DOI: 10.1016/S0167-8140(00)00245-0]
49 **Jordan BF**, Sonveaux P. Targeting tumor perfusion and oxygenation to improve the outcome of anticancer therapy. *Front Pharmacol* 2012; **3**: 94 [PMID: 22661950]
50 **Overgaard J**, Hansen HS, Overgaard M, Bastholt L, Berthelsen A, Specht L, Lindelov B, Jorgensen K. A randomized double-blind phase III study of nimorazole as a hypoxic radiosensitizer of primary radiotherapy in supraglottic larynx and pharynx carcinoma. Results of the Danish Head and Neck Cancer Study (DAHANCA) Protocol 5-85. *Radiother Oncol* 1998; **46**: 135-146 [DOI: 10.1016/S0167-8140(97)00220-X]
51 **Bentzen SM**. Theragnostic imaging for radiation oncology: dose-painting by numbers. *Lancet Oncol* 2005; **6**: 112-117 [DOI: 10.1016/S1470-2045(05)01737-7]
52 **Brown JM**, Workman P. Partition coefficient as a guide to the development of radiosensitizers which are less toxic than misonidazole. *Radiat Res* 1980; **82**: 171-190 [DOI: 10.2307/3575246]
53 **Chapman JD**. The detection and measurement of hypoxic cells in solid tumors. *Cancer* 1984; **54**: 2441-2449 [DOI: 10.1002/1097-0142(19841201)54: 11<2441: : AID-CNCR2820541122>3.0.CO; 2-S]
54 **Krohn KA,** Link JM, Mason RP. Molecular imaging of hypoxia. *J Nucl Med* 2008; **49** Suppl 2: 129S-148S
55 **Bruehlmeier M**, Roelcke U, Schubiger PA, Ametamey SM. Assessment of hypoxia and perfusion in human brain tumors using PET with 18F-fluoromisonidazole and 15O-H2O. *J Nucl Med* 2004; **45**: 1851-1859 [PMID: 15534054]
56 **Wang W**, Lee NY, Georgi JC, Narayanan M, Guillem J, Schöder H, Humm JL. Pharmacokinetic analysis of hypoxia (18)F-fluoromisonidazole dynamic PET in head and neck cancer. *J Nucl Med* 2010; **51**: 37-45 [PMID: 20008982 DOI: 10.2967/jnumed.109.067009]
57 **Sorger D**, Patt M, Kumar P, Wiebe LI, Barthel H, Seese A, Dannenberg C, Tannapfel A, Kluge R, Sabri O.

[18F]Fluoroazomycinarabinofuranoside (18FAZA) and [18F]Fluoromisonidazole (18FMISO): a comparative study of their selective uptake in hypoxic cells and PET imaging in experimental rat tumors. *Nucl Med Biol* 2003; **30**: 317-326 [DOI: 10.1016/S0969-8051(02)00442-0]

58 **Trinkaus ME**, Blum R, Rischin D, Callahan J, Bressel M, Segard T, Roselt P, Eu P, Binns D, MacManus MP, Ball D, Hicks RJ. Imaging of hypoxia with 18F-FAZA PET in patients with locally advanced non-small cell lung cancer treated with definitive chemoradiotherapy. *J Med Imaging Radiat Oncol* 2013; **57**: 475-481 [PMID: 23870348 DOI: 10.1111/1754-9485.12086]

59 **Verwer EE**, van Velden FH, Bahce I, Yaqub M, Schuit RC, Windhorst AD, Raijmakers P, Lammertsma AA, Smit EF, Boellaard R. Pharmacokinetic analysis of [18F]FAZA in non-small cell lung cancer patients. *Eur J Nucl Med Mol Imaging* 2013; **40**: 1523-1531 [PMID: 23740374 DOI: 10.1007/s00259-013-2462-3]

60 **Yang DJ**, Wallace S, Cherif A, Li C, Gretzer MB, Kim EE, Podoloff DA. Development of F-18-labeled fluoroerythronitroimidazole as a PET agent for imaging tumor hypoxia. *Radiology* 1995; **194**: 795-800 [PMID: 7862981]

61 **Dubois LJ**, Lieuwes NG, Janssen MH, Peeters WJ, Windhorst AD, Walsh JC, Kolb HC, Ollers MC, Bussink J, van Dongen GA, van der Kogel A, Lambin P. Preclinical evaluation and validation of [18F]HX4, a promising hypoxia marker for PET imaging. *Proc Natl Acad Sci USA* 2011; **108**: 14620-14625 [PMID: 21873245 DOI: 10.1073/pnas.1102526108]

62 **Petering HG**, Buskirk HH, Underwood GE. The anti-tumor activity of 2-keto-3-ethoxybutyraldehyde bis(thiosemicarbazone) and related compoundsS. *Cancer Res* 1964: 24367-24372

63 **Paterson BM**, Donnelly PS. Copper complexes of bis (thiosemicarbazones): from chemotherapeutics to diagnostic and therapeutic radiopharmaceuticals. *Chem Soc Rev* 2011; **40**: 3005-3018 [PMID: 21409228 DOI: 10.1039/c0cs00215a]

64 **Lewis J**, Laforest R, Buettner T, Song S, Fujibayashi Y, Connett J, Welch M. Copper-64-diacetyl-bis(N4-methylthiosemicarbazone): An agent for radiotherapy. *Proc Natl Acad Sci USA* 2001; **98**: 1206-1211 [PMID: 11158618 DOI: 10.1073/pnas.98.3.1206]

65 **Obata A**, Kasamatsu S, Lewis JS, Furukawa T, Takamatsu S, Toyohara J, Asai T, Welch MJ, Adams SG, Saji H, Yonekura Y, Fujibayashi Y. Basic characterization of 64Cu-ATSM as a radiotherapy agent. *Nucl Med Biol* 2005; **32**: 21-28 [PMID: 15691658 DOI: 10.1016/j.nucmedbio.2004.08.012]

66 **McCall KC**, Humm JL, Bartlett R, Reese M, Carlin S. Copper-64-diacetyl-bis(N(4)-methylthiosemicarbazone) pharmacokinetics in FaDu xenograft tumors and correlation with microscopic markers of hypoxia. *Int J Radiat Oncol Biol Phys* 2012; **84**: e393-e399 [PMID: 22727887 DOI: 10.1016/j.ijrobp.2012.05.005]

67 **Lohith TG**, Kudo T, Demura Y, Umeda Y, Kiyono Y, Fujibayashi Y, Okazawa H. Pathophysiologic correlation between 62Cu-ATSM and 18F-FDG in lung cancer. *J Nucl Med* 2009; **50**: 1948-1953 [PMID: 19910425 DOI: 10.2967/jnumed.109.069021]

68 **Dearling JL**, Packard AB. Some thoughts on the mechanism of cellular trapping of Cu(II)-ATSM. *Nucl Med Biol* 2010; **37**: 237-243 [PMID: 20346863 DOI: 10.1016/j.nucmedbio.2009.11.004]

69 **Vāvere AL**, Lewis JS. Cu-ATSM: a radiopharmaceutical for the PET imaging of hypoxia. *Dalton Trans* 2007; **(43)**: 4893-4902 [PMID: 17992274 DOI: 10.1039/b705989b]

70 **Basken NE**, Mathias CJ, Lipka AE, Green MA. Species dependence of [64Cu]Cu-Bis(thiosemicarbazone) radiopharmaceutical binding to serum albumins. *Nucl Med Biol* 2008; **35**: 281-286 [PMID: 18355683 DOI: 10.1016/j.nucmedbio.2007.11.009]

71 **Burgman P**, O'Donoghue JA, Lewis JS, Welch MJ, Humm JL, Ling CC. Cell line-dependent differences in uptake and retention of the hypoxia-selective nuclear imaging agent Cu-ATSM. *Nucl Med Biol* 2005; **32**: 623-630 [PMID: 16026709 DOI: 10.1016/j.nucmedbio.2005.05.003]

72 **O'Donoghue JA**, Zanzonico P, Pugachev A, Wen B, Smith-Jones P, Cai S, Burnazi E, Finn RD, Burgman P, Ruan S, Lewis JS, Welch MJ, Ling CC, Humm JL. Assessment of regional tumor hypoxia using 18F-fluoromisonidazole and 64Cu(II)-diacetyl-bis(N4-methylthiosemicarbazone) positron emission tomography: Comparative study featuring microPET imaging, Po2 probe measurement, autoradiography, and fluorescent microscopy in the R3327-AT and FaDu rat tumor models. *Int J Radiat Oncol Biol Phys* 2005; **61**: 1493-1502 [PMID: 15817355 DOI: 10.1016/j.ijrobp.2004.12.057]

73 **Liu J**, Hajibeigi A, Ren G, Lin M, Siyambalapitiyage W, Liu Z, Simpson E, Parkey RW, Sun X, Oz OK. Retention of the radiotracers 64Cu-ATSM and 64Cu-PTSM in human and murine tumors is influenced by MDR1 protein expression. *J Nucl Med* 2009; **50**: 1332-1339 [PMID: 19617332 DOI: 10.2967/jnumed.109.061879]

74 **Oh M**, Tanaka T, Kobayashi M, Furukawa T, Mori T, Kudo T, Fujieda S, Fujibayashi Y. Radio-copper-labeled Cu-ATSM: an indicator of quiescent but clonogenic cells under mild hypoxia in a Lewis lung carcinoma model. *Nucl Med Biol* 2009; **36**: 419-426 [PMID: 19423010 DOI: 10.1016/j.nucmedbio.2009.01.016]

75 **Yoshii Y**, Furukawa T, Kiyono Y, Watanabe R, Waki A, Mori T, Yoshii H, Oh M, Asai T, Okazawa H, Welch MJ, Fujibayashi Y. Copper-64-diacetyl-bis (N4-methylthiosemicarbazone) accumulates in rich regions of CD133+ highly tumorigenic cells in mouse colon carcinoma. *Nucl Med Biol* 2010; **37**: 395-404 [PMID: 20447549 DOI: 10.1016/j.nucmedbio.2009.12.011]

76 **Yoshii Y**, Yoneda M, Ikawa M, Furukawa T, Kiyono Y, Mori T, Yoshii H, Oyama N, Okazawa H, Saga T, Fujibayashi Y. Radiolabeled Cu-ATSM as a novel indicator of overreduced intracellular state due to mitochondrial dysfunction: studies with mitochondrial DNA-less ρ0 cells and cybrids carrying MELAS mitochondrial DNA mutation. *Nucl Med Biol* 2012; **39**: 177-185 [PMID: 22033022 DOI: 10.1016/j.nucmedbio.2011.08.008]

77 **Eschmann SM**, Paulsen F, Reimold M, Dittmann H, Welz S, Reischl G, Machulla HJ, Bares R. Prognostic impact of hypoxia imaging with 18F-misonidazole PET in non-small cell lung cancer and head and neck cancer before radiotherapy. *J Nucl Med* 2005; **46**: 253-260 [PMID: 15695784]

78 **Zegers CM**, van Elmpt W, Wierts R, Reymen B, Sharifi H, Öllers MC, Hoebers F, Troost EG, Wanders R, van Baardwijk A, Brans B, Eriksson J, Windhorst B, Mottaghy FM, De Ruysscher D, Lambin P. Hypoxia imaging with [^{18}F]HX4 PET in NSCLC patients: defining optimal imaging parameters. *Radiother Oncol* 2013; **109**: 58-64 [PMID: 24044790 DOI: 10.1016/j.radonc.2013.08.031]

79 **Takahashi N**, Fujibayashi Y, Yonekura Y, Welch MJ, Waki A, Tsuchida T, Sadato N, Sugimoto K, Itoh H. Evaluation of 62Cu labeled diacetyl-bis(N4-methylthiosemicarbazone) as a hypoxic tissue tracer in patients with lung cancer. *Ann Nucl Med* 2000; **14**: 323-328 [PMID: 11108159 DOI: 10.1007/BF02988690]

80 **Wong TZ**, Lacy JL, Petry NA, Hawk TC, Sporn TA, Dewhirst MW, Vlahovic G. PET of hypoxia and perfusion with 62Cu-ATSM and 62Cu-PTSM using a 62Zn/62Cu generator. *AJR Am J Roentgenol* 2008; **190**: 427-432 [PMID: 18212229 DOI: 10.2214/AJR.07.2876]

81 **Zhang T**, Das SK, Fels DR, Hansen KS, Wong TZ, Dewhirst MW, Vlahovic G. PET with 62Cu-ATSM and 62Cu-PTSM is a useful imaging tool for hypoxia and perfusion in pulmonary lesions. *AJR Am J Roentgenol* 2013; **201**: W698-W706 [PMID: 24147499 DOI: 10.2214/AJR.12.9698]

82 **Gagel B**, Reinartz P, Demirel C, Kaiser HJ, Zimny M, Piroth M, Pinkawa M, Stanzel S, Asadpour B, Hamacher K,

Coenen HH, Buell U, Eble MJ. [18F] fluoromisonidazole and [18F] fluorodeoxyglucose positron emission tomography in response evaluation after chemo-/radiotherapy of non-small-cell lung cancer: a feasibility study. *BMC Cancer* 2006; 651

83 **Vera P**, Bohn P, Edet-Sanson A, Salles A, Hapdey S, Gardin I, Ménard JF, Modzelewski R, Thiberville L, Dubray B. Simultaneous positron emission tomography (PET) assessment of metabolism with ^{18}F-fluoro-2-deoxy-d-glucose (FDG), proliferation with ^{18}F-fluoro-thymidine (FLT), and hypoxia with ^{18}fluoro-misonidazole (F-miso) before and during radiotherapy in patients with non-small-cell lung cancer (NSCLC): a pilot study. *Radiother Oncol* 2011; **98**: 109-116 [PMID: 21056487 DOI: 10.1016/j.radonc.2010.10.011]

84 **Li L**, Hu M, Zhu H, Zhao W, Yang G, Yu J. Comparison of 18F-Fluoroerythronitroimidazole and 18F-fluorodeoxyglucose positron emission tomography and prognostic value in locally advanced non-small-cell lung cancer. *Clin Lung Cancer* 2010; **11**: 335-340 [PMID: 20837459 DOI: 10.3816/CLC.2010.n.042]

85 **Hu M**, Xing L, Mu D, Yang W, Yang G, Kong L, Yu J. Hypoxia imaging with 18F-fluoroerythronitroimidazole integrated PET/CT and immunohistochemical studies in non-small cell lung cancer. *Clin Nucl Med* 2013; **38**: 591-596 [PMID: 23797219 DOI: 10.1097/RLU.0b013e318279fd3d]

86 **Dehdashti F**, Mintun MA, Lewis JS, Bradley J, Govindan R, Laforest R, Welch MJ, Siegel BA. In vivo assessment of tumor hypoxia in lung cancer with 60Cu-ATSM. *Eur J Nucl Med Mol Imaging* 2003; **30**: 844-850 [PMID: 12692685 DOI: 10.1007/s00259-003-1130-4]

87 **Koh WJ,** Bergman KS, Rasey JS, Peterson LM, Evans ML, Graham MM, Grierson JR, Lindsley KL, Lewellen TK, Krohn KA, Griffin TW. Evaluation of oxygenation status during fractionated radiotherapy in human nonsmall cell lung cancers using [F-18]fluoromisonidazole positron emission tomography. *Int J Radiat Oncol Biol Phys* 1995; **33**: 391-398 [DOI: 10.1016/0360-3016(95)00170-4]

88 **Ferrara N**, Gerber HP, LeCouter J. The biology of VEGF and its receptors. *Nat Med* 2003; **9**: 669-676 [PMID: 12778165 DOI: 10.1038/nm0603-669]

89 **Kerbel RS**. Tumor angiogenesis. *N Engl J Med* 2008; **358**: 2039-2049 [PMID: 18463380 DOI: 10.1056/NEJMra0706596]

90 **Ferrara N**, Hillan KJ, Gerber HP, Novotny W. Discovery and development of bevacizumab, an anti-VEGF antibody for treating cancer. *Nat Rev Drug Discov* 2004; **3**: 391-400 [PMID: 15136787 DOI: 10.1038/nrd1381]

91 **van der Veldt AA**, Haanen JB, van den Eertwegh AJ, Boven E. Targeted therapy for renal cell cancer: current perspectives. *Discov Med* 2010; **10**: 394-405 [PMID: 21122471]

92 **Laking G**, Price P. Radionuclide imaging of perfusion and hypoxia. *Eur J Nucl Med Mol Imaging* 2010; **37** Suppl 1: S20-S29

93 **Gupta A**, DiFilippo FP, Brunken RC. Rubidium-82 uptake in metastases from pheochromocytoma on PET myocardial perfusion images. *Clin Nucl Med* 2011; **36**: 930-931 [PMID: 21892051 DOI: 10.1097/RLU.0b013e31822920b7]

94 **Xiangsong Z**, Xinjian W, Yong Z, Weian C. 13N-NH3: a selective contrast-enhancing tracer for brain tumor. *Nucl Med Commun* 2008; **29**: 1052-1058 [PMID: 18987525 DOI: 10.1097/MNM.0b013e328310af34]

95 **de Langen AJ**, van den Boogaart VE, Marcus JT, Lubberink M. Use of H2(15)O-PET and DCE-MRI to measure tumor blood flow. *Oncologist* 2008; **13**: 631-644 [PMID: 18586918 DOI: 10.1634/theoncologist.2007-0235]

96 **Herscovitch P**, Markham J, Raichle ME. Brain blood flow measured with intravenous H2(15)O. I. Theory and error analysis. *J Nucl Med* 1983; **24**: 782-789 [PMID: 6604139]

97 **Hoekstra CJ**, Stroobants SG, Hoekstra OS, Smit EF, Vansteenkiste JF, Lammertsma AA. Measurement of perfusion in stage IIIA-N2 non-small cell lung cancer using H(2)(15)O and positron emission tomography. *Clin Cancer Res* 2002; **8**: 2109-2115 [PMID: 12114410]

98 **Kubo S**, Yamamoto K, Magata Y, Iwasaki Y, Tamaki N, Yonekura Y, Konishi J. Assessment of pancreatic blood flow with positron emission tomography and oxygen-15 water. *Ann Nucl Med* 1991; **5**: 133-138 [PMID: 1797067 DOI: 10.1007/BF03164627]

99 **Lehtiö K**, Oikonen V, Grönroos T, Eskola O, Kalliokoski K, Bergman J, Solin O, Grénman R, Nuutila P, Minn H. Imaging of blood flow and hypoxia in head and neck cancer: initial evaluation with [(15)O]H(2)O and [(18)F]fluoroerythronitroimidazole PET. *J Nucl Med* 2001; **42**: 1643-1652 [PMID: 11696633]

100 **Lodge MA**, Carson RE, Carrasquillo JA, Whatley M, Libutti SK, Bacharach SL. Parametric images of blood flow in oncology PET studies using [15O]water. *J Nucl Med* 2000; **41**: 1784-1792 [PMID: 11079484]

101 **Wilson CB**, Lammertsma AA, McKenzie CG, Sikora K, Jones T. Measurements of blood flow and exchanging water space in breast tumors using positron emission tomography: a rapid and noninvasive dynamic method. *Cancer Res* 1992; **52**: 1592-1597 [PMID: 1540969]

102 **Schuster DP**, Markham J, Welch MJ. Positron emission tomography measurements of pulmonary vascular permeability with Ga-68 transferrin or C-11 methylalbumin. *Crit Care Med* 1998; **26**: 518-525 [PMID: 9504581 DOI: 10.1097/00003246-199803000-00026]

103 **Brooks DJ**, Frackowiak RS, Lammertsma AA, Herold S, Leenders KL, Selwyn AP, Turton DR, Brady F, Jones T. A comparison between regional cerebral blood flow measurements obtained in human subjects using 11C-methylalbumin microspheres, the C15O2 steady-state method, and positron emission tomography. *Acta Neurol Scand* 1986; **73**: 415-422 [PMID: 3088902 DOI: 10.1111/j.1600-0404.1986.tb03298.x]

104 **de Langen AJ**, Lubberink M, Boellaard R, Spreeuwenberg MD, Smit EF, Hoekstra OS, Lammertsma AA. Reproducibility of tumor perfusion measurements using 15O-labeled water and PET. *J Nucl Med* 2008; **49**: 1763-1768 [PMID: 18927324 DOI: 10.2967/jnumed.108.053454]

105 **van der Veldt AA**, Hendrikse NH, Harms HJ, Comans EF, Postmus PE, Smit EF, Lammertsma AA, Lubberink M. Quantitative parametric perfusion images using 15O-labeled water and a clinical PET/CT scanner: test-retest variability in lung cancer. *J Nucl Med* 2010; **51**: 1684-1690 [PMID: 20956480 DOI: 10.2967/jnumed.110.079137]

106 **Shi K**, Souvatzoglou M, Astner ST, Vaupel P, Nüsslin F, Wilkens JJ, Ziegler SI. Quantitative assessment of hypoxia kinetic models by a cross-study of dynamic 18F-FAZA and 15O-H2O in patients with head and neck tumors. *J Nucl Med* 2010; **51**: 1386-1394 [PMID: 20720045 DOI: 10.2967/jnumed.109.074336]

107 **Anderson H**, Yap JT, Wells P, Miller MP, Propper D, Price P, Harris AL. Measurement of renal tumour and normal tissue perfusion using positron emission tomography in a phase II clinical trial of razoxane. *Br J Cancer* 2003; **89**: 262-267 [PMID: 12865914 DOI: 10.1038/sj.bjc.6601105]

108 **Anderson HL**, Yap JT, Miller MP, Robbins A, Jones T, Price PM. Assessment of pharmacodynamic vascular response in a phase I trial of combretastatin A4 phosphate. *J Clin Oncol* 2003; **21**: 2823-2830 [PMID: 12807935 DOI: 10.1200/JCO.2003.05.186]

109 **Herbst RS**, Mullani NA, Davis DW, Hess KR, McConkey DJ, Charnsangavej C, O'Reilly MS, Kim HW, Baker C, Roach J, Ellis LM, Rashid A, Pluda J, Bucana C, Madden TL, Tran HT, Abbruzzese JL. Development of biologic markers of response and assessment of antiangiogenic activity in a clinical trial of human recombinant endostatin. *J Clin Oncol* 2002; **20**: 3804-3814 [PMID: 12228200 DOI: 10.1200/JCO.2002.05.102]

110 **Lara PN**, Quinn DI, Margolin K, Meyers FJ, Longmate J, Frankel P, Mack PC, Turrell C, Valk P, Rao J, Buckley P, Wun T, Gosselin R, Galvin I, Gumerlock PH, Lenz HJ, Doroshow JH, Gandara DR. SU5416 plus interferon alpha in advanced renal cell carcinoma: a phase II California Cancer Consortium Study with biological and imaging correlates of angiogenesis inhibition. *Clin Cancer Res* 2003; **9**: 4772-4781 [PMID: 14581348]

111 **de Langen AJ**, van den Boogaart V, Lubberink M, Backes WH, Marcus JT, van Tinteren H, Pruim J, Brans B, Leffers P, Dingemans AM, Smit EF, Groen HJ, Hoekstra OS. Monitoring response to antiangiogenic therapy in non-small cell lung cancer using imaging markers derived from PET and dynamic contrast-enhanced MRI. *J Nucl Med* 2011; **52**: 48-55 [PMID: 21149474 DOI: 10.2967/jnumed.110.078261]

112 **Eisenhauer EA**, Therasse P, Bogaerts J, Schwartz LH, Sargent D, Ford R, Dancey J, Arbuck S, Gwyther S, Mooney M, Rubinstein L, Shankar L, Dodd L, Kaplan R, Lacombe D, Verweij J. New response evaluation criteria in solid tumours: revised RECIST guideline (version 1.1). *Eur J Cancer* 2009; **45**: 228-247 [PMID: 19097774 DOI: 10.1016/j.ejca.2008.10.026]

113 **Van der Veldt AA**, Lubberink M, Bahce I, Walraven M, de Boer MP, Greuter HN, Hendrikse NH, Eriksson J, Windhorst AD, Postmus PE, Verheul HM, Serné EH, Lammertsma AA, Smit EF. Rapid decrease in delivery of chemotherapy to tumors after anti-VEGF therapy: implications for scheduling of anti-angiogenic drugs. *Cancer Cell* 2012; **21**: 82-91 [PMID: 22264790 DOI: 10.1016/j.ccr.2011.11.023]

114 **van der Veldt AA**, Luurtsema G, Lubberink M, Lammertsma AA, Hendrikse NH. Individualized treatment planning in oncology: role of PET and radiolabelled anticancer drugs in predicting tumour resistance. *Curr Pharm Des* 2008; **14**: 2914-2931 [PMID: 18991710 DOI: 10.2174/138161208786404344]

115 **van der Veldt AA**, Smit EF, Lammertsma AA. Cancer therapy: could a novel test predict the amount of drug that reaches its target? *Expert Rev Anticancer Ther* 2013; **13**: 377-379 [PMID: 23560831 DOI: 10.1586/era.13.13]

116 **Dimitrakopoulou A**, Strauss LG, Clorius JH, Ostertag H, Schlag P, Heim M, Oberdorfer F, Helus F, Haberkorn U, van Kaick G. Studies with positron emission tomography after systemic administration of fluorine-18-uracil in patients with liver metastases from colorectal carcinoma. *J Nucl Med* 1993; **34**: 1075-1081 [PMID: 8315481]

117 **Gupta N**, Saleem A, Kötz B, Osman S, Aboagye EO, Phillips R, Vernon C, Wasan H, Jones T, Hoskin PJ, Price PM. Carbogen and nicotinamide increase blood flow and 5-fluorouracil delivery but not 5-fluorouracil retention in colorectal cancer metastases in patients. *Clin Cancer Res* 2006; **12**: 3115-3123 [PMID: 16707610 DOI: 10.1158/1078-0432.CCR-05-0513]

118 **Harte RJ**, Matthews JC, O'Reilly SM, Tilsley DW, Osman S, Brown G, Luthra SJ, Brady F, Jones T, Price PM. Tumor, normal tissue, and plasma pharmacokinetic studies of fluorouracil biomodulation with N-phosphonacetyl-L-aspartate, folinic acid, and interferon alfa. *J Clin Oncol* 1999; **17**: 1580-1588 [PMID: 10334547]

119 **Saleem A**, Harte RJ, Matthews JC, Osman S, Brady F, Luthra SK, Brown GD, Bleehen N, Connors T, Jones T, Price PM, Aboagye EO. Pharmacokinetic evaluation of N-[2-(dimethylamino)ethyl]acridine-4-carboxamide in patients by positron emission tomography. *J Clin Oncol* 2001; **19**: 1421-1429 [PMID: 11230487]

120 **van der Veldt AA**, Lubberink M, Greuter HN, Comans EF, Herder GJ, Yaqub M, Schuit RC, van Lingen A, Rizvi SN, Mooijer MP, Rijnders AY, Windhorst AD, Smit EF, Hendrikse NH, Lammertsma AA. Absolute quantification of [(11)C]docetaxel kinetics in lung cancer patients using positron emission tomography. *Clin Cancer Res* 2011; **17**: 4814-4824 [PMID: 21750197 DOI: 10.1158/1078-0432.CCR-10-2933]

121 **van der Veldt AA**, Lubberink M, Mathijssen RH, Loos WJ, Herder GJ, Greuter HN, Comans EF, Rutten HB, Eriksson J, Windhorst AD, Hendrikse NH, Postmus PE, Smit EF, Lammertsma AA. Toward prediction of efficacy of chemotherapy: a proof of concept study in lung cancer patients using [^{11}C]docetaxel and positron emission tomography. *Clin Cancer Res* 2013; **19**: 4163-4173 [PMID: 23620410 DOI: 10.1158/1078-0432.CCR-12-3779]

122 **Saleem A**, Price PM. Early tumor drug pharmacokinetics is influenced by tumor perfusion but not plasma drug exposure. *Clin Cancer Res* 2008; **14**: 8184-8190 [PMID: 19088034 DOI: 10.1158/1078-0432.CCR-08-1324]

123 **Van der Veldt AA**, Lammertsma AA, Smit EF. Scheduling of anticancer drugs: timing may be everything. *Cell Cycle* 2012; **11**: 4339-4343 [PMID: 23032365 DOI: 10.4161/cc.22187]

124 **Zimny M**, Gagel B, DiMartino E, Hamacher K, Coenen HH, Westhofen M, Eble M, Buell U, Reinartz P. FDG--a marker of tumour hypoxia? A comparison with [18F]fluoromisonidazole and pO2-polarography in metastatic head and neck cancer. *Eur J Nucl Med Mol Imaging* 2006; **33**: 1426-1431 [PMID: 16841141 DOI: 10.1007/s00259-006-0175-6]

125 **Bentzen L**, Keiding S, Nordsmark M, Falborg L, Hansen SB, Keller J, Nielsen OS, Overgaard J. Tumour oxygenation assessed by 18F-fluoromisonidazole PET and polarographic needle electrodes in human soft tissue tumours. *Radiother Oncol* 2003; **67**: 339-344 [DOI: 10.1016/S0167-8140(03)00081-1]

126 **Gagel B**, Reinartz P, Dimartino E, Zimny M, Pinkawa M, Maneschi P, Stanzel S, Hamacher K, Coenen HH, Westhofen M, Büll U, Eble MJ. pO(2) Polarography versus positron emission tomography ([(18)F] fluoromisonidazole, [(18)F]-2-fluoro-2'-deoxyglucose). An appraisal of radiotherapeutically relevant hypoxia. *Strahlenther Onkol* 2004; **180**: 616-622 [PMID: 15480509 DOI: 10.1007/s00066-004-1229-y]

127 **Mortensen LS**, Buus S, Nordsmark M, Bentzen L, Munk OL, Keiding S, Overgaard J. Identifying hypoxia in human tumors: A correlation study between 18F-FMISO PET and the Eppendorf oxygen-sensitive electrode. *Acta Oncol* 2010; **49**: 934-940 [PMID: 20831480 DOI: 10.3109/0284186X.2010.516274]

128 **Dewhirst MW**, Cao Y, Moeller B. Cycling hypoxia and free radicals regulate angiogenesis and radiotherapy response. *Nat Rev Cancer* 2008; **8**: 425-437 [PMID: 18500244 DOI: 10.1038/nrc2397]

129 **Jain RK**. Normalization of tumor vasculature: an emerging concept in antiangiogenic therapy. *Science* 2005; **307**: 58-62 [PMID: 15637262 DOI: 10.1126/science.1104819]

130 **Lee CG**, Heijn M, di Tomaso E, Griffon-Etienne G, Ancukiewicz M, Koike C, Park KR, Ferrara N, Jain RK, Suit HD, Boucher Y. Anti-Vascular endothelial growth factor treatment augments tumor radiation response under normoxic or hypoxic conditions. *Cancer Res* 2000; **60**: 5565-5570 [PMID: 11034104]

131 **Hugonnet F**, Fournier L, Medioni J, Smadja C, Hindié E, Huchet V, Itti E, Cuenod CA, Chatellier G, Oudard S, Faraggi M. Metastatic renal cell carcinoma: relationship between initial metastasis hypoxia, change after 1 month's sunitinib, and therapeutic response: an 18F-fluoromisonidazole PET/CT study. *J Nucl Med* 2011; **52**: 1048-1055 [PMID: 21680694 DOI: 10.2967/jnumed.110.084517]

132 **Murakami M**, Zhao S, Zhao Y, Chowdhury NF, Yu W, Nishijima K, Takiguchi M, Tamaki N, Kuge Y. Evaluation of changes in the tumor microenvironment after sorafenib therapy by sequential histology and 18F-fluoromisonidazole hypoxia imaging in renal cell carcinoma. *Int J Oncol* 2012; **41**: 1593-1600 [PMID: 22965141]

133 **Lewis JS**, Sharp TL, Laforest R, Fujibayashi Y, Welch MJ. Tumor uptake of copper-diacetyl-bis(N(4)-methylthiosemi-

carbazone): effect of changes in tissue oxygenation. *J Nucl Med* 2001; **42**: 655-661 [PMID: 11337556]
134 **Yuan H**, Schroeder T, Bowsher JE, Hedlund LW, Wong T, Dewhirst MW. Intertumoral differences in hypoxia selectivity of the PET imaging agent 64Cu(II)-diacetyl-bis(N4-methylthiosemicarbazone). *J Nucl Med* 2006; **47**: 989-998 [PMID: 16741309]
135 **Kersemans V**, Cornelissen B, Hueting R, Tredwell M, Hussien K, Allen PD, Falzone N, Hill SA, Dilworth JR, Gouverneur V, Muschel RJ, Smart SC. Hypoxia imaging using PET and SPECT: the effects of anesthetic and carrier gas on [Cu]-ATSM, [Tc]-HL91 and [F]-FMISO tumor hypoxia accumulation. *PLoS One* 2011; **6**: e25911 [PMID: 22102855 DOI: 10.1371/journal.pone.0025911]
136 **Matsumoto K**, Szajek L, Krishna MC, Cook JA, Seidel J, Grimes K, Carson J, Sowers AL, English S, Green MV, Bacharach SL, Eckelman WC, Mitchell JB. The influence of tumor oxygenation on hypoxia imaging in murine squamous cell carcinoma using [64Cu]Cu-ATSM or [18F]Fluoromisonidazole positron emission tomography. *Int J Oncol* 2007; **30**: 873-881 [PMID: 17332926]
137 **Ballegeer EA**, Madrill NJ, Berger KL, Agnew DW, McNiel EA. Evaluation of hypoxia in a feline model of head and neck cancer using (6)(4)Cu-ATSM positron emission tomography/computed tomography. *BMC Cancer* 2013: 13218
138 **Bowen SR**, van der Kogel AJ, Nordsmark M, Bentzen SM, Jeraj R. Characterization of positron emission tomography hypoxia tracer uptake and tissue oxygenation via electrochemical modeling. *Nucl Med Biol* 2011; **38**: 771-780 [PMID: 21843774 DOI: 10.1016/j.nucmedbio.2011.02.002]
139 **Myerson RJ**, Singh AK, Bigott HM, Cha B, Engelbach JA, Kim J, Lamoreaux WT, Moros E, Novak P, Sharp TL, Straube W, Welch MJ, Xu M. Monitoring the effect of mild hyperthermia on tumour hypoxia by Cu-ATSM PET scanning. *Int J Hyperthermia* 2006; **22**: 93-115 [PMID: 16754595 DOI: 10.1080/02656730600594191]
140 **Hansen AE,** Kristensen AT, Jorgensen JT, McEvoy FJ, Busk M, van der Kogel AJ, Bussink J, Engelholm SA, Kjaer A. (64)Cu-ATSM and (18)FDG PET uptake and (64)Cu-ATSM autoradiography in spontaneous canine tumors: comparison with pimonidazole hypoxia immunohistochemistry. *Radiat Oncol* 2012: 789
141 **Grigsby PW**, Malyapa RS, Higashikubo R, Schwarz JK, Welch MJ, Huettner PC, Dehdashti F. Comparison of molecular markers of hypoxia and imaging with (60)Cu-ATSM in cancer of the uterine cervix. *Mol Imaging Biol* 2007; **9**: 278-283 [PMID: 17431727 DOI: 10.1007/s11307-007-0095-2]
142 **Tateishi K**, Tateishi U, Sato M, Yamanaka S, Kanno H, Murata H, Inoue T, Kawahara N. Application of 62Cu-diacetyl-bis (N4-methylthiosemicarbazone) PET imaging to predict highly malignant tumor grades and hypoxia-inducible factor-1α expression in patients with glioma. *AJNR Am J Neuroradiol* 2013; **34**: 92-99 [PMID: 22700754 DOI: 10.3174/ajnr.A3159]
143 **Valtorta S**, Belloli S, Sanvito F, Masiello V, Di Grigoli G, Monterisi C, Fazio F, Picchio M, Moresco RM. Comparison of 18F-fluoroazomycin-arabinofuranoside and 64Cu-diacetyl-bis(N4-methylthiosemicarbazone) in preclinical models of cancer. *J Nucl Med* 2013; **54**: 1106-1112 [PMID: 23699667 DOI: 10.2967/jnumed.112.111120]
144 **Weeks AJ**, Paul RL, Marsden PK, Blower PJ, Lloyd DR. Radiobiological effects of hypoxia-dependent uptake of 64Cu-ATSM: enhanced DNA damage and cytotoxicity in hypoxic cells. *Eur J Nucl Med Mol Imaging* 2010; **37**: 330-338 [PMID: 19915836 DOI: 10.1007/s00259-009-1305-8]
145 **Dence CS**, Ponde DE, Welch MJ, Lewis JS. Autoradiographic and small-animal PET comparisons between (18)F-FMISO, (18)F-FDG, (18)F-FLT and the hypoxic selective (64)Cu-ATSM in a rodent model of cancer. *Nucl Med Biol* 2008; **35**: 713-720 [PMID: 18678357 DOI: 10.1016/j.nucmedbio.2008.06.001]
146 **Lewis JS**, McCarthy DW, McCarthy TJ, Fujibayashi Y, Welch MJ. Evaluation of 64Cu-ATSM in vitro and in vivo in a hypoxic tumor model. *J Nucl Med* 1999; **40**: 177-183 [PMID: 9935074]
147 **Chao KS,** Bosch WR, Mutic S, Lewis JS, Dehdashti F, Mintun MA, Dempsey JF, Perez CA, Purdy JA, Welch MJ. A novel approach to overcome hypoxic tumor resistance: Cu-ATSM-guided intensity-modulated radiation therapy. *Int J Radiat Oncol Biol Phys* 2001; **49**: 1171-1182 [DOI: 10.1016/S0360-3016(00)01433-4]
148 **Dehdashti F,** Grigsby PW, Mintun MA, Lewis JS, Siegel BA, Welch MJ. Assessing tumor hypoxia in cervical cancer by positron emission tomography with 60Cu-ATSM: relationship to therapeutic response-a preliminary report. *Int J Radiat Oncol Biol Phys* 2003; **55**: 1233-1238 [DOI: 10.1016/S0360-3016(02)04477-2]
149 **Dehdashti F**, Grigsby PW, Lewis JS, Laforest R, Siegel BA, Welch MJ. Assessing tumor hypoxia in cervical cancer by PET with 60Cu-labeled diacetyl-bis(N4-methylthiosemicarbazone). *J Nucl Med* 2008; **49**: 201-205 [PMID: 18199612 DOI: 10.2967/jnumed.107.048520]
150 **Dietz DW**, Dehdashti F, Grigsby PW, Malyapa RS, Myerson RJ, Picus J, Ritter J, Lewis JS, Welch MJ, Siegel BA. Tumor hypoxia detected by positron emission tomography with 60Cu-ATSM as a predictor of response and survival in patients undergoing Neoadjuvant chemoradiotherapy for rectal carcinoma: a pilot study. *Dis Colon Rectum* 2008; **51**: 1641-1648 [PMID: 18682881 DOI: 10.1007/s10350-008-9420-3]
151 **Grassi I**, Nanni C, Cicoria G, Blasi C, Bunkheila F, Lopci E, Colletti PM, Rubello D, Fanti S. Usefulness of 64Cu-ATSM in Head and Neck Cancer: A Preliminary Prospective Study. *Clin Nucl Med* 2013
152 **Kositwattanarerk A**, Oh M, Kudo T, Kiyono Y, Mori T, Kimura Y, Maruyama R, Fujibayashi Y, Fujieda S, Okazawa H. Different distribution of (62) Cu ATSM and (18)F-FDG in head and neck cancers. *Clin Nucl Med* 2012; **37**: 252-257 [PMID: 22310251 DOI: 10.1097/RLU.0b013e31823eaadb]
153 **Laforest R**, Dehdashti F, Lewis JS, Schwarz SW. Dosimetry of 60/61/62/64Cu-ATSM: a hypoxia imaging agent for PET. *Eur J Nucl Med Mol Imaging* 2005; **32**: 764-770 [PMID: 15785955 DOI: 10.1007/s00259-004-1756-x]
154 **Lewis JS**, Laforest R, Dehdashti F, Grigsby PW, Welch MJ, Siegel BA. An imaging comparison of 64Cu-ATSM and 60Cu-ATSM in cancer of the uterine cervix. *J Nucl Med* 2008; **49**: 1177-1182 [PMID: 18552145 DOI: 10.2967/jnumed.108.051326]
155 **Minagawa Y**, Shizukuishi K, Koike I, Horiuchi C, Watanuki K, Hata M, Omura M, Odagiri K, Tohnai I, Inoue T, Tateishi U. Assessment of tumor hypoxia by 62Cu-ATSM PET/CT as a predictor of response in head and neck cancer: a pilot study. *Ann Nucl Med* 2011; **25**: 339-345 [PMID: 21327756 DOI: 10.1007/s12149-011-0471-5]
156 **Nyflot MJ**, Harari PM, Yip S, Perlman SB, Jeraj R. Correlation of PET images of metabolism, proliferation and hypoxia to characterize tumor phenotype in patients with cancer of the oropharynx. *Radiother Oncol* 2012; **105**: 36-40 [PMID: 23068711 DOI: 10.1016/j.radonc.2012.09.012]
157 **Evans SM**, Kachur AV, Shiue CY, Hustinx R, Jenkins WT, Shive GG, Karp JS, Alavi A, Lord EM, Dolbier WR, Koch CJ. Noninvasive detection of tumor hypoxia using the 2-nitroimidazole [18F]EF1. *J Nucl Med* 2000; **41**: 327-336 [PMID: 10688119]
158 **Mahy P**, De Bast M, de Groot T, Cheguillaume A, Gillart J, Haustermans K, Labar D, Grégoire V. Comparative pharmacokinetics, biodistribution, metabolism and hypoxia-dependent uptake of [18F]-EF3 and [18F]-MISO in rodent tumor models. *Radiother Oncol* 2008; **89**: 353-360 [PMID: 18649964 DOI: 10.1016/j.radonc.2008.06.008]
159 **Mahy P**, De Bast M, Gillart J, Labar D, Grégoire V. Detection

of tumour hypoxia: comparison between EF5 adducts and [18F]EF3 uptake on an individual mouse tumour basis. *Eur J Nucl Med Mol Imaging* 2006; **33**: 553-556 [PMID: 16523307 DOI: 10.1007/s00259-005-0049-3]

160 **Dubois L**, Landuyt W, Cloetens L, Bol A, Bormans G, Haustermans K, Labar D, Nuyts J, Grégoire V, Mortelmans L. [18F]EF3 is not superior to [18F]FMISO for PET-based hypoxia evaluation as measured in a rat rhabdomyosarcoma tumour model. *Eur J Nucl Med Mol Imaging* 2009; **36**: 209-218 [PMID: 18690432 DOI: 10.1007/s00259-008-0907-x]

161 **Mahy P**, Geets X, Lonneux M, Levêque P, Christian N, De Bast M, Gillart J, Labar D, Lee J, Grégoire V. Determination of tumour hypoxia with [18F]EF3 in patients with head and neck tumours: a phase I study to assess the tracer pharmacokinetics, biodistribution and metabolism. *Eur J Nucl Med Mol Imaging* 2008; **35**: 1282-1289 [PMID: 18317752 DOI: 10.1007/s00259-008-0742-0]

162 **Yapp DT**, Woo J, Kartono A, Sy J, Oliver T, Skov KA, Koch CJ, Adomat H, Dragowska WH, Fazli L, Ruth T, Adam MJ, Green D, Gleave M. Non-invasive evaluation of tumour hypoxia in the Shionogi tumour model for prostate cancer with 18F-EF5 and positron emission tomography. *BJU Int* 2007; **99**: 1154-1160 [PMID: 17309552 DOI: 10.1111/j.1464-410X.2007.06761.x]

163 **Ziemer LS**, Evans SM, Kachur AV, Shuman AL, Cardi CA, Jenkins WT, Karp JS, Alavi A, Dolbier WR, Koch CJ. Noninvasive imaging of tumor hypoxia in rats using the 2-nitroimidazole 18F-EF5. *Eur J Nucl Med Mol Imaging* 2003; **30**: 259-266 [PMID: 12552344 DOI: 10.1007/s00259-002-1037-5]

164 **Komar G**, Seppänen M, Eskola O, Lindholm P, Grönroos TJ, Forsback S, Sipilä H, Evans SM, Solin O, Minn H. 18F-EF5: a new PET tracer for imaging hypoxia in head and neck cancer. *J Nucl Med* 2008; **49**: 1944-1951 [PMID: 18997048 DOI: 10.2967/jnumed.108.053785]

165 **Reischl G**, Dorow DS, Cullinane C, Katsifis A, Roselt P, Binns D, Hicks RJ. Imaging of tumor hypoxia with [124I]IAZA in comparison with [18F]FMISO and [18F]FAZA--first small animal PET results. *J Pharm Pharm Sci* 2007; **10**: 203-211 [PMID: 17706178]

166 **Piert M**, Machulla HJ, Picchio M, Reischl G, Ziegler S, Kumar P, Wester HJ, Beck R, McEwan AJ, Wiebe LI, Schwaiger M. Hypoxia-specific tumor imaging with 18F-fluoroazomycin arabinoside. *J Nucl Med* 2005; **46**: 106-113 [PMID: 15632040]

167 **Picchio M**, Beck R, Haubner R, Seidl S, Machulla HJ, Johnson TD, Wester HJ, Reischl G, Schwaiger M, Piert M. Intratumoral spatial distribution of hypoxia and angiogenesis assessed by 18F-FAZA and 125I-Gluco-RGD autoradiography. *J Nucl Med* 2008; **49**: 597-605 [PMID: 18344437 DOI: 10.2967/jnumed.107.046870]

168 **Maier FC**, Kneilling M, Reischl G, Cay F, Bukala D, Schmid A, Judenhofer MS, Rocken M, Machulla HJ, Pichler BJ. Significant impact of different oxygen breathing conditions on noninvasive in vivo tumor-hypoxia imaging using [(1)(8)F]-fluoro-azomycinarabino-furanoside ([(1)(8)F]FAZA). *Radiat Oncol* 2011: 6165

169 **Tran LB**, Bol A, Labar D, Jordan B, Magat J, Mignion L, Grégoire V, Gallez B. Hypoxia imaging with the nitroimidazole 18F-FAZA PET tracer: a comparison with OxyLite, EPR oximetry and 19F-MRI relaxometry. *Radiother Oncol* 2012; **105**: 29-35 [PMID: 22677038 DOI: 10.1016/j.radonc.2012.04.011]

170 **Busk M**, Horsman MR, Jakobsen S, Keiding S, van der Kogel AJ, Bussink J, Overgaard J. Imaging hypoxia in xenografted and murine tumors with 18F-fluoroazomycin arabinoside: a comparative study involving microPET, autoradiography, PO2-polarography, and fluorescence microscopy. *Int J Radiat Oncol Biol Phys* 2008; **70**: 1202-1212 [PMID: 18313528 DOI: 10.1016/j.ijrobp.2007.11.034]

171 **Mortensen LS**, Busk M, Nordsmark M, Jakobsen S, Theil J, Overgaard J, Horsman MR. Accessing radiation response using hypoxia PET imaging and oxygen sensitive electrodes: a preclinical study. *Radiother Oncol* 2011; **99**: 418-423 [PMID: 21723634 DOI: 10.1016/j.radonc.2011.06.034]

172 **Busk M**, Horsman MR, Jakobsen S, Hansen KV, Bussink J, van der Kogel A, Overgaard J. Can hypoxia-PET map hypoxic cell density heterogeneity accurately in an animal tumor model at a clinically obtainable image contrast? *Radiother Oncol* 2009; **92**: 429-436 [PMID: 19729214 DOI: 10.1016/j.radonc.2009.08.026]

173 **Busk M**, Munk OL, Jakobsen S, Wang T, Skals M, Steiniche T, Horsman MR, Overgaard J. Assessing hypoxia in animal tumor models based on pharmocokinetic analysis of dynamic FAZA PET. *Acta Oncol* 2010; **49**: 922-933 [PMID: 20831479 DOI: 10.3109/0284186X.2010.503970]

174 **Busk M**, Jakobsen S, Horsman MR, Mortensen LS, Iversen AB, Overgaard J, Nordsmark M, Ji X, Lee DY, Raleigh JR. PET imaging of tumor hypoxia using 18F-labeled pimonidazole. *Acta Oncol* 2013; **52**: 1300-1307 [PMID: 23962243 DOI: 10.3109/0284186X.2013.815797]

175 **Busk M**, Mortensen LS, Nordsmark M, Overgaard J, Jakobsen S, Hansen KV, Theil J, Kallehauge JF, D'Andrea FP, Steiniche T, Horsman MR. PET hypoxia imaging with FAZA: reproducibility at baseline and during fractionated radiotherapy in tumour-bearing mice. *Eur J Nucl Med Mol Imaging* 2013; **40**: 186-197 [PMID: 23076620 DOI: 10.1007/s00259-012-2258-x]

176 **Graves EE**, Vilalta M, Cecic IK, Erler JT, Tran PT, Felsher D, Sayles L, Sweet-Cordero A, Le QT, Giaccia AJ. Hypoxia in models of lung cancer: implications for targeted therapeutics. *Clin Cancer Res* 2010; **16**: 4843-4852 [PMID: 20858837 DOI: 10.1158/1078-0432.CCR-10-1206]

177 **Solomon B**, Binns D, Roselt P, Weibe LI, McArthur GA, Cullinane C, Hicks RJ. Modulation of intratumoral hypoxia by the epidermal growth factor receptor inhibitor gefitinib detected using small animal PET imaging. *Mol Cancer Ther* 2005; **4**: 1417-1422 [PMID: 16170034 DOI: 10.1158/1535-7163.MCT-05-0066]

178 **Belloli S**, Brioschi A, Politi LS, Ronchetti F, Calderoni S, Raccagni I, Pagani A, Monterisi C, Zenga F, Zara G, Fazio F, Mauro A, Moresco RM. Characterization of biological features of a rat F98 GBM model: a PET-MRI study with [18F]FAZA and [18F]FDG. *Nucl Med Biol* 2013; **40**: 831-840 [PMID: 23915802 DOI: 10.1016/j.nucmedbio.2013.05.004]

179 **Troost EG**, Laverman P, Kaanders JH, Oyen WJ, Boerman OC, Bussink J. Intratumoral spatial distribution of hypoxia and angiogenesis assessed by 18F-FAZA and 125I-gluco-RGD autoradiography. *J Nucl Med* 2008; **49**: 1732; author reply 1732-1733 [PMID: 18794277 DOI: 10.2967/jnumed.108.053777]

180 **Postema EJ**, McEwan AJ, Riauka TA, Kumar P, Richmond DA, Abrams DN, Wiebe LI. Initial results of hypoxia imaging using 1-alpha-D: -(5-deoxy-5-[18F]-fluoroarabinofuranosyl)-2-nitroimidazole (18F-FAZA). *Eur J Nucl Med Mol Imaging* 2009; **36**: 1565-1573 [PMID: 19430784 DOI: 10.1007/s00259-009-1154-5]

181 **Bollineni VR**, Kerner GS, Pruim J, Steenbakkers RJ, Wiegman EM, Koole MJ, de Groot EH, Willemsen AT, Luurtsema G, Widder J, Groen HJ, Langendijk JA. PET imaging of tumor hypoxia using 18F-fluoroazomycin arabinoside in stage III-IV non-small cell lung cancer patients. *J Nucl Med* 2013; **54**: 1175-1180 [PMID: 23753185 DOI: 10.2967/jnumed.112.115014]

182 **Grosu AL**, Souvatzoglou M, Röper B, Dobritz M, Wiedenmann N, Jacob V, Wester HJ, Reischl G, Machulla HJ, Schwaiger M, Molls M, Piert M. Hypoxia imaging with FAZA-PET and theoretical considerations with regard to dose painting for individualization of radiotherapy in patients with head and neck cancer. *Int J Radiat Oncol Biol Phys* 2007; **69**: 541-551 [PMID: 17869667 DOI: 10.1016/j.ijrobp.2007.05.079]

183 **Souvatzoglou M**, Grosu AL, Röper B, Krause BJ, Beck R, Reischl G, Picchio M, Machulla HJ, Wester HJ, Piert M. Tumour hypoxia imaging with [18F]FAZA PET in head and neck cancer patients: a pilot study. *Eur J Nucl Med Mol Imaging* 2007; **34**: 1566-1575 [PMID: 17447061 DOI: 10.1007/s00259-007-0424-3]

184 **Schuetz M**, Schmid MP, Pötter R, Kommata S, Georg D, Lukic D, Dudczak R, Kletter K, Dimopoulos J, Karanikas G, Bachtiary B. Evaluating repetitive 18F-fluoroazomycin-arabinoside (18FAZA) PET in the setting of MRI guided adaptive radiotherapy in cervical cancer. *Acta Oncol* 2010; **49**: 941-947 [PMID: 20831481 DOI: 10.3109/0284186X.2010.510145]

185 **Mortensen LS**, Johansen J, Kallehauge J, Primdahl H, Busk M, Lassen P, Alsner J, Sørensen BS, Toustrup K, Jakobsen S, Petersen J, Petersen H, Theil J, Nordsmark M, Overgaard J. FAZA PET/CT hypoxia imaging in patients with squamous cell carcinoma of the head and neck treated with radiotherapy: results from the DAHANCA 24 trial. *Radiother Oncol* 2012; **105**: 14-20 [PMID: 23083497 DOI: 10.1016/j.radonc.2012.09.015]

186 **Havelund BM**, Holdgaard PC, Rafaelsen SR, Mortensen LS, Theil J, Bender D, Pløen J, Spindler KL, Jakobsen A. Tumour hypoxia imaging with 18F-fluoroazomycinarabinofuranoside PET/CT in patients with locally advanced rectal cancer. *Nucl Med Commun* 2013; **34**: 155-161 [PMID: 23196674 DOI: 10.1097/MNM.0b013e32835bd5bc]

187 **Barthel H**, Wilson H, Collingridge DR, Brown G, Osman S, Luthra SK, Brady F, Workman P, Price PM, Aboagye EO. In vivo evaluation of [18F]fluoroetanidazole as a new marker for imaging tumour hypoxia with positron emission tomography. *Br J Cancer* 2004; **90**: 2232-2242 [PMID: 15150578]

188 **Rasey JS**, Hofstrand PD, Chin LK, Tewson TJ. Characterization of [18F]fluoroetanidazole, a new radiopharmaceutical for detecting tumor hypoxia. *J Nucl Med* 1999; **40**: 1072-1079 [PMID: 10452326]

189 **Grönroos T**, Bentzen L, Marjamäki P, Murata R, Horsman MR, Keiding S, Eskola O, Haaparanta M, Minn H, Solin O. Comparison of the biodistribution of two hypoxia markers [18F]FETNIM and [18F]FMISO in an experimental mammary carcinoma. *Eur J Nucl Med Mol Imaging* 2004; **31**: 513-520 [PMID: 14722675 DOI: 10.1007/s00259-003-1404-x]

190 **Tolvanen T**, Lehtiö K, Kulmala J, Oikonen V, Eskola O, Bergman J, Minn H. 18F-Fluoroerythronitroimidazole radiation dosimetry in cancer studies. *J Nucl Med* 2002; **43**: 1674-1680 [PMID: 12468519]

191 **Lehtiö K**, Oikonen V, Nyman S, Grönroos T, Roivainen A, Eskola O, Minn H. Quantifying tumour hypoxia with fluorine-18 fluoroerythronitroimidazole ([18F]FETNIM) and PET using the tumour to plasma ratio. *Eur J Nucl Med Mol Imaging* 2003; **30**: 101-108 [PMID: 12483416 DOI: 10.1007/s00259-002-1016-x]

192 **Lehtiö K**, Eskola O, Viljanen T, Oikonen V, Grönroos T, Sillanmäki L, Grénman R, Minn H. Imaging perfusion and hypoxia with PET to predict radiotherapy response in head-and-neck cancer. *Int J Radiat Oncol Biol Phys* 2004; **59**: 971-982 [PMID: 15234030 DOI: 10.1016/j.ijrobp.2003.12.014]

193 **Vercellino L**, Groheux D, Thoury A, Delord M, Schlageter MH, Delpech Y, Barré E, Baruch-Hennequin V, Tylski P, Homyrda L, Walker F, Barranger E, Hindié E. Hypoxia imaging of uterine cervix carcinoma with (18)F-FETNIM PET/CT. *Clin Nucl Med* 2012; **37**: 1065-1068 [PMID: 22996235 DOI: 10.1097/RLU.0b013e3182638e7e]

194 **Yue J**, Yang Y, Cabrera AR, Sun X, Zhao S, Xie P, Zheng J, Ma L, Fu Z, Yu J. Measuring tumor hypoxia with ^{18}F-FETNIM PET in esophageal squamous cell carcinoma: a pilot clinical study. *Dis Esophagus* 2012; **25**: 54-61 [PMID: 21595781 DOI: 10.1111/j.1442-2050.2011.01209.x]

195 **Bentzen L**, Keiding S, Horsman MR, Falborg L, Hansen SB, Overgaard J. Feasibility of detecting hypoxia in experimental mouse tumours with 18F-fluorinated tracers and positron emission tomography--a study evaluating [18F]Fluoro-2-deoxy-D-glucose. *Acta Oncol* 2000; **39**: 629-637 [PMID: 11093372 DOI: 10.1080/028418600750013320]

196 **Rasey JS,** Casciari JJ, Hofstrand PD, Muzi M, Graham MM, Chin LK. Determining hypoxic fraction in a rat glioma by uptake of radiolabeled fluoromisonidazole. *Radiat Res* 2000; **153**: 84-92 [DOI: 10.1667/0033-7587(2000)153[0084:DHFIAR]2.0.CO; 2]

197 **Bentzen L**, Keiding S, Horsman MR, Grönroos T, Hansen SB, Overgaard J. Assessment of hypoxia in experimental mice tumours by [18F]fluoromisonidazole PET and pO2 electrode measurements. Influence of tumour volume and carbogen breathing. *Acta Oncol* 2002; **41**: 304-312 [PMID: 12195751 DOI: 10.1080/02841860260088863]

198 **Troost EG**, Laverman P, Kaanders JH, Philippens M, Lok J, Oyen WJ, van der Kogel AJ, Boerman OC, Bussink J. Imaging hypoxia after oxygenation-modification: comparing [18F]FMISO autoradiography with pimonidazole immunohistochemistry in human xenograft tumors. *Radiother Oncol* 2006; **80**: 157-164 [PMID: 16905213 DOI: 10.1016/j.radonc.2006.07.023]

199 **Bruehlmeier M**, Kaser-Hotz B, Achermann R, Bley CR, Wergin M, Schubiger PA, Ametamey SM. Measurement of tumor hypoxia in spontaneous canine sarcomas. *Vet Radiol Ultrasound* 2005; **46**: 348-354 [PMID: 16229439 DOI: 10.1111/j.1740-8261.2005.00065.x]

200 **Lawrentschuk N**, Poon AM, Foo SS, Putra LG, Murone C, Davis ID, Bolton DM, Scott AM. Assessing regional hypoxia in human renal tumours using 18F-fluoromisonidazole positron emission tomography. *BJU Int* 2005; **96**: 540-546 [PMID: 16104907 DOI: 10.1111/j.1464-410X.2005.05681.x]

201 **Sørensen M**, Horsman MR, Cumming P, Munk OL, Keiding S. Effect of intratumoral heterogeneity in oxygenation status on FMISO PET, autoradiography, and electrode Po2 measurements in murine tumors. *Int J Radiat Oncol Biol Phys* 2005; **62**: 854-861 [PMID: 15936570 DOI: 10.1016/j.ijrobp.2005.02.044]

202 **Gagel B,** Piroth M, Pinkawa M, Reinartz P, Zimny M, Kaiser HJ, Stanzel S, Asadpour B, Demirel C, Hamacher K, Coenen HH, Scholbach T, Maneschi P, DiMartino E, Eble MJ. pO polarography, contrast enhanced color duplex sonography (CDS), [18F] fluoromisonidazole and [18F] fluorodeoxyglucose positron emission tomography: validated methods for the evaluation of therapy-relevant tumor oxygenation or only bricks in the puzzle of tumor hypoxia? *BMC Cancer* 2007: 7113

203 **Carlin S**, Pugachev A, Sun X, Burke S, Claus F, O'Donoghue J, Ling CC, Humm JL. In vivo characterization of a reporter gene system for imaging hypoxia-induced gene expression. *Nucl Med Biol* 2009; **36**: 821-831 [PMID: 19720294 DOI: 10.1016/j.nucmedbio.2009.06.006]

204 **Chang J**, Wen B, Kazanzides P, Zanzonico P, Finn RD, Fichtinger G, Ling CC. A robotic system for 18F-FMISO PET-guided intratumoral pO2 measurements. *Med Phys* 2009; **36**: 5301-5309 [PMID: 19994538 DOI: 10.1118/1.3239491]

205 **Hatano T**, Zhao S, Zhao Y, Nishijima K, Kuno N, Hanzawa H, Sakamoto T, Tamaki N, Kuge Y. Biological characteristics of intratumoral [F-18]-fluoromisonidazole distribution in a rodent model of glioma. *Int J Oncol* 2013; **42**: 823-830 [PMID: 23338175]

206 **Huang T**, Civelek AC, Zheng H, Ng CK, Duan X, Li J, Postel GC, Shen B, Li XF. (18)F-misonidazole PET imaging of hypoxia in micrometastases and macroscopic xenografts of human non-small cell lung cancer: a correlation with autoradiography and histological findings. *Am J Nucl Med Mol Imaging* 2013; **3**: 142-153 [PMID: 23526377]

207 **Huang T**, Civelek AC, Li J, Jiang H, Ng CK, Postel GC, Shen B, Li XF. Tumor microenvironment-dependent 18F-FDG, 18F-fluorothymidine, and 18F-misonidazole uptake: a pilot study in mouse models of human non-small cell lung can-

cer. *J Nucl Med* 2012; **53**: 1262-1268 [PMID: 22717978 DOI: 10.2967/jnumed.111.098087]
208 **Oehler C**, O'Donoghue JA, Russell J, Zanzonico P, Lorenzen S, Ling CC, Carlin S. 18F-fluromisonidazole PET imaging as a biomarker for the response to 5,6-dimethylxanthenone-4-acetic acid in colorectal xenograft tumors. *J Nucl Med* 2011; **52**: 437-444 [PMID: 21321262 DOI: 10.2967/jnumed.110.081372]
209 **Cho H**, Ackerstaff E, Carlin S, Lupu ME, Wang Y, Rizwan A, O'Donoghue J, Ling CC, Humm JL, Zanzonico PB, Koutcher JA. Noninvasive multimodality imaging of the tumor microenvironment: registered dynamic magnetic resonance imaging and positron emission tomography studies of a preclinical tumor model of tumor hypoxia. *Neoplasia* 2009; **11**: 247-259, 2p
210 **Troost EG**, Laverman P, Philippens ME, Lok J, van der Kogel AJ, Oyen WJ, Boerman OC, Kaanders JH, Bussink J. Correlation of [18F]FMISO autoradiography and pimonidazole [corrected] immunohistochemistry in human head and neck carcinoma xenografts. *Eur J Nucl Med Mol Imaging* 2008; **35**: 1803-1811 [PMID: 18421457 DOI: 10.1007/s00259-008-0772-7]
211 **Dubois L**, Landuyt W, Haustermans K, Dupont P, Bormans G, Vermaelen P, Flamen P, Verbeken E, Mortelmans L. Evaluation of hypoxia in an experimental rat tumour model by [(18)F]fluoromisonidazole PET and immunohistochemistry. *Br J Cancer* 2004; **91**: 1947-1954 [PMID: 15520822 DOI: 10.1038/sj.bjc.6602219]
212 **Cherk MH**, Foo SS, Poon AM, Knight SR, Murone C, Papenfuss AT, Sachinidis JI, Saunder TH, O'Keefe GJ, Scott AM. Lack of correlation of hypoxic cell fraction and angiogenesis with glucose metabolic rate in non-small cell lung cancer assessed by 18F-Fluoromisonidazole and 18F-FDG PET. *J Nucl Med* 2006; **47**: 1921-1926 [PMID: 17138734]
213 **Riesterer O**, Honer M, Jochum W, Oehler C, Ametamey S, Pruschy M. Ionizing radiation antagonizes tumor hypoxia induced by antiangiogenic treatment. *Clin Cancer Res* 2006; **12**: 3518-3524 [PMID: 16740778 DOI: 10.1158/1078-0432.CCR-05-2816]
214 **Lehmann S**, Stiehl DP, Honer M, Dominietto M, Keist R, Kotevic I, Wollenick K, Ametamey S, Wenger RH, Rudin M. Longitudinal and multimodal in vivo imaging of tumor hypoxia and its downstream molecular events. *Proc Natl Acad Sci USA* 2009; **106**: 14004-14009 [PMID: 19666490 DOI: 10.1073/pnas.0901194106]
215 **Chen L**, Zhang Z, Kolb HC, Walsh JC, Zhang J, Guan Y. ^{18}F-HX4 hypoxia imaging with PET/CT in head and neck cancer: a comparison with ^{18}F-FMISO. *Nucl Med Commun* 2012; **33**: 1096-1102 [PMID: 22836736 DOI: 10.1097/MNM.0b013e3283571016]
216 **Campanile C**, Arlt MJ, Krämer SD, Honer M, Gvozdenovic A, Brennecke P, Fischer CR, Sabile AA, Müller A, Ametamey SM, Born W, Schibli R, Fuchs B. Characterization of different osteosarcoma phenotypes by PET imaging in preclinical animal models. *J Nucl Med* 2013; **54**: 1362-1368 [PMID: 23801674 DOI: 10.2967/jnumed.112.115527]
217 **Cheng J**, Lei L, Xu J, Sun Y, Zhang Y, Wang X, Pan L, Shao Z, Zhang Y, Liu G. 18F-fluoromisonidazole PET/CT: a potential tool for predicting primary endocrine therapy resistance in breast cancer. *J Nucl Med* 2013; **54**: 333-340 [PMID: 23401605 DOI: 10.2967/jnumed.112.111963]
218 **Sato J**, Kitagawa Y, Yamazaki Y, Hata H, Okamoto S, Shiga T, Shindoh M, Kuge Y, Tamaki N. 18F-fluoromisonidazole PET uptake is correlated with hypoxia-inducible factor-1α expression in oral squamous cell carcinoma. *J Nucl Med* 2013; **54**: 1060-1065 [PMID: 23699668 DOI: 10.2967/jnumed.112.114355]
219 **Norikane T**, Yamamoto Y, Maeda Y, Kudomi N, Matsunaga T, Haba R, Iwasaki A, Hoshikawa H, Nishiyama Y. Correlation of (18)F-fluoromisonidazole PET findings with HIF-1α and p53 expressions in head and neck cancer: comparison with (18)F-FDG PET. *Nucl Med Commun* 2014; **35**: 30-35 [PMID: 24121312 DOI: 10.1097/MNM.0000000000000010]
220 **Rasey JS**, Koh WJ, Evans ML, Peterson LM, Lewellen TK, Graham MM, Krohn KA. Quantifying regional hypoxia in human tumors with positron emission tomography of [18F]fluoromisonidazole: a pretherapy study of 37 patients. *Int J Radiat Oncol Biol Phys* 1996; **36**: 417-428 [DOI: 10.1016/S0360-3016(96)00325-2]
221 **Koh WJ**, Rasey JS, Evans ML, Grierson JR, Lewellen TK, Graham MM, Krohn KA, Griffin TW. Imaging of hypoxia in human tumors with [F-18]fluoromisonidazole. *Int J Radiat Oncol Biol Phys* 1992; **22**: 199-212 [DOI: 10.1016/0360-3016(92)91001-4]
222 **Liu RS**, Chu LS, Yen SH, Chang CP, Chou KL, Wu LC, Chang CW, Lui MT, Chen KY, Yeh SH. Detection of anaerobic odontogenic infections by fluorine-18 fluoromisonidazole. *Eur J Nucl Med* 1996; **23**: 1384-1387 [PMID: 8781145 DOI: 10.1007/BF01367596]
223 **Yeh SH**, Liu RS, Wu LC, Yang DJ, Yen SH, Chang CW, Yu TW, Chou KL, Chen KY. Fluorine-18 fluoromisonidazole tumour to muscle retention ratio for the detection of hypoxia in nasopharyngeal carcinoma. *Eur J Nucl Med* 1996; **23**: 1378-1383 [PMID: 8781144 DOI: 10.1007/BF01367595]
224 **Rischin D**, Peters L, Hicks R, Hughes P, Fisher R, Hart R, Sexton M, D'Costa I, von Roemeling R. Phase I trial of concurrent tirapazamine, cisplatin, and radiotherapy in patients with advanced head and neck cancer. *J Clin Oncol* 2001; **19**: 535-542 [PMID: 11208848]
225 **Rajendran JG**, Wilson DC, Conrad EU, Peterson LM, Bruckner JD, Rasey JS, Chin LK, Hofstrand PD, Grierson JR, Eary JF, Krohn KA. [(18)F]FMISO and [(18)F]FDG PET imaging in soft tissue sarcomas: correlation of hypoxia, metabolism and VEGF expression. *Eur J Nucl Med Mol Imaging* 2003; **30**: 695-704 [PMID: 12632200 DOI: 10.1007/s00259-002-1096-7]
226 **Rajendran JG**, Mankoff DA, O'Sullivan F, Peterson LM, Schwartz DL, Conrad EU, Spence AM, Muzi M, Farwell DG, Krohn KA. Hypoxia and glucose metabolism in malignant tumors: evaluation by [18F]fluoromisonidazole and [18F]fluorodeoxyglucose positron emission tomography imaging. *Clin Cancer Res* 2004; **10**: 2245-2252 [PMID: 15073099 DOI: 10.1158/1078-0432.CCR-0688-3]
227 **Hicks RJ**, Rischin D, Fisher R, Binns D, Scott AM, Peters LJ. Utility of FMISO PET in advanced head and neck cancer treated with chemoradiation incorporating a hypoxia-targeting chemotherapy agent. *Eur J Nucl Med Mol Imaging* 2005; **32**: 1384-1391 [PMID: 16133382 DOI: 10.1007/s00259-005-1880-2]
228 **Loi S**, Ngan SY, Hicks RJ, Mukesh B, Mitchell P, Michael M, Zalcberg J, Leong T, Lim-Joon D, Mackay J, Rischin D. Oxaliplatin combined with infusional 5-fluorouracil and concomitant radiotherapy in inoperable and metastatic rectal cancer: a phase I trial. *Br J Cancer* 2005; **92**: 655-661 [PMID: 15700033 DOI: 10.1038/sj.bjc.6602413]
229 **Thorwarth D**, Eschmann SM, Scheiderbauer J, Paulsen F, Alber M. Kinetic analysis of dynamic 18F-fluoromisonidazole PET correlates with radiation treatment outcome in head-and-neck cancer. *BMC Cancer* 2005: 5152
230 **Rajendran JG**, Schwartz DL, O'Sullivan J, Peterson LM, Ng P, Scharnhorst J, Grierson JR, Krohn KA. Tumor hypoxia imaging with [F-18] fluoromisonidazole positron emission tomography in head and neck cancer. *Clin Cancer Res* 2006; **12**: 5435-5441 [PMID: 17000677 DOI: 10.1158/1078-0432.CCR-05-1773]
231 **Rischin D**, Hicks RJ, Fisher R, Binns D, Corry J, Porceddu S, Peters LJ. Prognostic significance of [18F]-misonidazole positron emission tomography-detected tumor hypoxia in patients with advanced head and neck cancer randomly assigned to chemoradiation with or without tirapaza-

mine: a substudy of Trans-Tasman Radiation Oncology Group Study 98.02. *J Clin Oncol* 2006; **24**: 2098-2104 [PMID: 16648512 DOI: 10.1200/JCO.2005.05.2878]

232 **Thorwarth D**, Eschmann SM, Holzner F, Paulsen F, Alber M. Combined uptake of [18F]FDG and [18F]FMISO correlates with radiation therapy outcome in head-and-neck cancer patients. *Radiother Oncol* 2006; **80**: 151-156 [PMID: 16920211 DOI: 10.1016/j.radonc.2006.07.033]

233 **Eschmann SM**, Paulsen F, Bedeshem C, Machulla HJ, Hehr T, Bamberg M, Bares R. Hypoxia-imaging with (18)F-Misonidazole and PET: changes of kinetics during radiotherapy of head-and-neck cancer. *Radiother Oncol* 2007; **83**: 406-410 [PMID: 17543402 DOI: 10.1016/j.radonc.2007.05.014]

234 **Thorwarth D**, Eschmann SM, Paulsen F, Alber M. A model of reoxygenation dynamics of head-and-neck tumors based on serial 18F-fluoromisonidazole positron emission tomography investigations. *Int J Radiat Oncol Biol Phys* 2007; **68**: 515-521 [PMID: 17398015 DOI: 10.1016/j.ijrobp.2006.12.037]

235 **Thorwarth D**, Eschmann SM, Paulsen F, Alber M. Hypoxia dose painting by numbers: a planning study. *Int J Radiat Oncol Biol Phys* 2007; **68**: 291-300 [PMID: 17448882 DOI: 10.1016/j.ijrobp.2006.11.061]

236 **Lee NY**, Mechalakos JG, Nehmeh S, Lin Z, Squire OD, Cai S, Chan K, Zanzonico PB, Greco C, Ling CC, Humm JL, Schöder H. Fluorine-18-labeled fluoromisonidazole positron emission and computed tomography-guided intensity-modulated radiotherapy for head and neck cancer: a feasibility study. *Int J Radiat Oncol Biol Phys* 2008; **70**: 2-13 [PMID: 17869020 DOI: 10.1016/j.ijrobp.2007.06.039]

237 **Lin Z**, Mechalakos J, Nehmeh S, Schoder H, Lee N, Humm J, Ling CC. The influence of changes in tumor hypoxia on dose-painting treatment plans based on 18F-FMISO positron emission tomography. *Int J Radiat Oncol Biol Phys* 2008; **70**: 1219-1228 [PMID: 18313529 DOI: 10.1016/j.ijrobp.2007.09.050]

238 **Nehmeh SA**, Lee NY, Schröder H, Squire O, Zanzonico PB, Erdi YE, Greco C, Mageras G, Pham HS, Larson SM, Ling CC, Humm JL. Reproducibility of intratumor distribution of (18)F-fluoromisonidazole in head and neck cancer. *Int J Radiat Oncol Biol Phys* 2008; **70**: 235-242 [PMID: 18086391 DOI: 10.1016/j.ijrobp.2007.08.036]

239 **Roels S**, Slagmolen P, Nuyts J, Lee JA, Loeckx D, Maes F, Stroobants S, Penninckx F, Haustermans K. Biological image-guided radiotherapy in rectal cancer: is there a role for FMISO or FLT, next to FDG? *Acta Oncol* 2008; **47**: 1237-1248 [PMID: 18654902 DOI: 10.1080/02841860802256434]

240 **Dirix P**, Vandecaveye V, De Keyzer F, Stroobants S, Hermans R, Nuyts S. Dose painting in radiotherapy for head and neck squamous cell carcinoma: value of repeated functional imaging with (18)F-FDG PET, (18)F-fluoromisonidazole PET, diffusion-weighted MRI, and dynamic contrast-enhanced MRI. *J Nucl Med* 2009; **50**: 1020-1027 [PMID: 19525447 DOI: 10.2967/jnumed.109.062638]

241 **Lee N**, Nehmeh S, Schöder H, Fury M, Chan K, Ling CC, Humm J. Prospective trial incorporating pre-/mid-treatment [18F]-misonidazole positron emission tomography for head-and-neck cancer patients undergoing concurrent chemoradiotherapy. *Int J Radiat Oncol Biol Phys* 2009; **75**: 101-108 [PMID: 19203843 DOI: 10.1016/j.ijrobp.2008.10.049]

242 **Abolmaali N**, Haase R, Koch A, Zips D, Steinbach J, Baumann M, Kotzerke J, Zöphel K. Two or four hour [^{18}F]FMISO-PET in HNSCC. When is the contrast best? *Nuklearmedizin* 2011; **50**: 22-27 [PMID: 21165537 DOI: 10.3413/nukmed-00328-10-07]

243 **Eary JF**, Link JM, Muzi M, Conrad EU, Mankoff DA, White JK, Krohn KA. Multiagent PET for risk characterization in sarcoma. *J Nucl Med* 2011; **52**: 541-546 [PMID: 21421714 DOI: 10.2967/jnumed.110.083717]

244 **Kikuchi M**, Yamane T, Shinohara S, Fujiwara K, Hori SY, Tona Y, Yamazaki H, Naito Y, Senda M. 18F-fluoromisonidazole positron emission tomography before treatment is a predictor of radiotherapy outcome and survival prognosis in patients with head and neck squamous cell carcinoma. *Ann Nucl Med* 2011; **25**: 625-633 [PMID: 21720778 DOI: 10.1007/s12149-011-0508-9]

245 **Yamane T**, Kikuchi M, Shinohara S, Senda M. Reduction of [(18)F]fluoromisonidazole uptake after neoadjuvant chemotherapy for head and neck squamous cell carcinoma. *Mol Imaging Biol* 2011; **13**: 227-231 [PMID: 20552284 DOI: 10.1007/s11307-010-0365-2]

246 **Mammar H**, Kerrou K, Nataf V, Pontvert D, Clemenceau S, Lot G, George B, Polivka M, Mokhtari K, Ferrand R, Feuvret L, Habrand JL, Pouysségur J, Mazure N, Talbot JN. Positron emission tomography/computed tomography imaging of residual skull base chordoma before radiotherapy using fluoromisonidazole and fluorodeoxyglucose: potential consequences for dose painting. *Int J Radiat Oncol Biol Phys* 2012; **84**: 681-687 [PMID: 22391104 DOI: 10.1016/j.ijrobp.2011.12.047]

247 **Zips D**, Zöphel K, Abolmaali N, Perrin R, Abramyuk A, Haase R, Appold S, Steinbach J, Kotzerke J, Baumann M. Exploratory prospective trial of hypoxia-specific PET imaging during radiochemotherapy in patients with locally advanced head-and-neck cancer. *Radiother Oncol* 2012; **105**: 21-28 [PMID: 23022173 DOI: 10.1016/j.radonc.2012.08.019]

248 **Henriques de Figueiredo B**, Merlin T, de Clermont-Gallerande H, Hatt M, Vimont D, Fernandez P, Lamare F. Potential of [18F]-fluoromisonidazole positron-emission tomography for radiotherapy planning in head and neck squamous cell carcinomas. *Strahlenther Onkol* 2013; **189**: 1015-1019 [PMID: 24173497 DOI: 10.1007/s00066-013-0454-7]

249 **Okamoto S**, Shiga T, Yasuda K, Ito YM, Magota K, Kasai K, Kuge Y, Shirato H, Tamaki N. High reproducibility of tumor hypoxia evaluated by 18F-fluoromisonidazole PET for head and neck cancer. *J Nucl Med* 2013; **54**: 201-207 [PMID: 23321456 DOI: 10.2967/jnumed.112.109330]

250 **Segard T**, Robins PD, Yusoff IF, Ee H, Morandeau L, Campbell EM, Francis RJ. Detection of hypoxia with 18F-fluoromisonidazole (18F-FMISO) PET/CT in suspected or proven pancreatic cancer. *Clin Nucl Med* 2013; **38**: 1-6 [PMID: 23242037 DOI: 10.1097/RLU.0b013e3182708777]

251 **Tachibana I**, Nishimura Y, Shibata T, Kanamori S, Nakamatsu K, Koike R, Nishikawa T, Ishikawa K, Tamura M, Hosono M. A prospective clinical trial of tumor hypoxia imaging with 18F-fluoromisonidazole positron emission tomography and computed tomography (F-MISO PET/CT) before and during radiation therapy. *J Radiat Res* 2013; **54**: 1078-1084 [PMID: 23589026 DOI: 10.1093/jrr/rrt033]

252 **Kaneta T**, Takai Y, Iwata R, Hakamatsuka T, Yasuda H, Nakayama K, Ishikawa Y, Watanuki S, Furumoto S, Funaki Y, Nakata E, Jingu K, Tsujitani M, Ito M, Fukuda H, Takahashi S, Yamada S. Initial evaluation of dynamic human imaging using 18F-FRP170 as a new PET tracer for imaging hypoxia. *Ann Nucl Med* 2007; **21**: 101-107 [PMID: 17424976 DOI: 10.1007/BF03033987]

253 **van Loon J**, Janssen MH, Ollers M, Aerts HJ, Dubois L, Hochstenbag M, Dingemans AM, Lalisang R, Brans B, Windhorst B, van Dongen GA, Kolb H, Zhang J, De Ruysscher D, Lambin P. PET imaging of hypoxia using [18F]HX4: a phase I trial. *Eur J Nucl Med Mol Imaging* 2010; **37**: 1663-1668 [PMID: 20369236 DOI: 10.1007/s00259-010-1437-x]

254 **Zanzonico P**, O'Donoghue J, Chapman JD, Schneider R, Cai S, Larson S, Wen B, Chen Y, Finn R, Ruan S, Gerweck L, Humm J, Ling C. Iodine-124-labeled iodo-azomycin-galactoside imaging of tumor hypoxia in mice with serial microPET scanning. *Eur J Nucl Med Mol Imaging* 2004; **31**: 117-128 [PMID: 14523586 DOI: 10.1007/s00259-003-1322-y]

255 **Riedl CC**, Brader P, Zanzonico P, Reid V, Woo Y, Wen B, Ling CC, Hricak H, Fong Y, Humm JL. Tumor hypoxia imaging in orthotopic liver tumors and peritoneal metasta-

sis: a comparative study featuring dynamic 18F-MISO and 124I-IAZG PET in the same study cohort. *Eur J Nucl Med Mol Imaging* 2008; **35**: 39-46 [PMID: 17786438 DOI: 10.1007/s00259-007-0522-2]

P- Reviewer: Hida T, Kawai H, Pereira-Vega A **S- Editor**: Ji FF
L- Editor: A **E- Editor**: Lu YJ

Published by **Baishideng Publishing Group Inc**
8226 Regency Drive, Pleasanton, CA 94588, USA
Telephone: +1-925-223-8242
Fax: +1-925-223-8243
E-mail: bpgoffice@wjgnet.com
Help Desk: http://www.wjgnet.com/esps/helpdesk.aspx
http://www.wjgnet.com